

CFD Analysis of Container Ship Sinkage, Trim and Resistance
(abridged)

Shaun Wortley

B. Eng. Mechanical Engineering
Project Report
Department of Mechanical Engineering
Curtin University

2013

21 Guillardon Tce,
Madora Bay,
WA 6210

8th November 2013

Professor Tilak Chandratilleke
Department of Mechanical Engineering,
Curtin University,
Kent Street,
Bentley,
WA 6102

Dear Sir,

I submit this report entitled CFD Analysis of Container Ship Sinkage, Trim and Resistance, based on Mechanical Project 491/493, undertaken by me as part-requirement for the degree of B. Eng. in Mechanical Engineering.

Yours Faithfully,

Shaun Wortley

Acknowledgements

I would like to thank Andrew King and Tim Gourlay for all their help and supervision throughout the project. Andrew your expertise and knowledge on all things CFD and numerical methods was never ending and you were able give good advice on how I could get the best results possible. Tim your wealth of knowledge and resources on marine design gave me that extra level for my project where my engineering awareness didn't always give me that understanding of the data obtained. I can definitely say that when I was truly baffled you both always had an appropriate answer to help me on my way, so again thank you.

I would also like to acknowledge iVEC's Epic supercomputing system for providing me with the processer power and memory to run the large simulations in OpenFOAM. These cases would have not been completed without this help.

Abstract

This report examined the effectiveness of the Computational Fluid Dynamics modeling software OpenFOAM in determining different hydrodynamic values for a container ship. The data that was calculated included squat (sinkage and trim) and resistance. The container ship dimensions were obtained from the Duisburg Test Case where for one case of draught 14.0m the waterline length was 361m, the beam was 51m and the displacement equaled 166124m³. A draught of 13.0m and 14.5m were also used and a scaled down version of the 14.0m draught according to the ratio 1:40. These ships were simulated in three different situations including a restricted stepped channel, deep and shallow water.

Container ships are constantly becoming larger and are required to carry more loads and travel at faster speeds. Therefore it is vital to the development of these huge structures that accurate methods of obtaining design data are established. Model testing in towing tanks is the past and present way of doing this for container ships. With computers reaching new levels and our understanding of CFD always improving, new and old programs require their accuracy in hydrodynamics to be determined. Hence the aims of the project were to use OpenFOAM to calculate the squat and resistance and compare this with benchmark experimental testing. There was not a large amount of experimental data available so other programs such as Maxsurf and Michlet were used to further compare and validate the accuracy of OpenFOAM. The squat was determined in the channel for all three draughts and speeds of 6, 10 and 14 knots. The viscous, wave and total resistance were calculated in deep and shallow water for two draughts and speeds ranging from 6 to 25 knots. And finally the model scale was simulated with the sinkage, trim and resistance values all being obtained for three speeds.

Meshing was done with utilities in OpenFOAM with the channel having roughly 0.36 million cells and deep water with 12 million cells. The system was set up with a multiphase volume of fluid method. The Reynolds Average Navier-Stokes equations were solved using a k- ω shear stress transport turbulent model and the LTSInterFoam solver which uses local

time stepping for multiphase situations. The simulations were run in parallel on iVEC's Epic system where the channel case took roughly 300CPU hours to solve and the deep water solved in 650CPU hours. Post-processing was mainly done by integrating the pressure over the surface of the hull and breaking the forces into their components.

The results were promising as they provided a good understanding of where OpenFOAM was accurate and where it had problems. The squat at an intermediate speed and draught in the channel was 24% higher than the experimental and 29% different in the scaled down version. All other values for squat were much larger except at the highest speeds simulated. The trim in the model scale was 11.3 times larger than the experimental. For all resistance calculations the wave resistance was mostly double the experimental data and the viscous was a minimum of 2% different in deep water and 54% in shallow water.

The conclusions made found that OpenFOAM was quite good at predicting the dynamic pressure for small clearances between the hull and seabed. However it overestimates the drag forces especially wave resistance, but was consistently accurate for viscous resistance. It was determined that the main reason for these errors was because of the very coarse mesh used in all simulations. However fine meshes required a large amount of computation time, so there had to be a balance between this and accuracy. Therefore it was recommended that the mesh be refined more in the areas around the bulb, rudder and free surface. Future work that could further this topic would include examining the differences between full and model scale simulations. Also modeling the ship in rough waters so as to calculate the heave, pitch and roll and other dynamic motions.

Table of Contents

Acknowledgements	iii
Abstract	v
Table of Contents	vii
List of Figures	ix
List of Tables	x
Nomenclature	xi
1.0 Introduction	1
1.1 Motivation for this Project	1
1.2 Objectives	2
1.3 Project Report Overview	3
5.0 CFD Modeling Approach in this Project	7
5.1 Geometry	8
5.1.1 Container Ship	8
5.1.2 Channel	9
5.1.3 Model Scale	10
5.2 Grid Generation and Meshing	11
5.3 Initial and Boundary Conditions	15
5.4 Flow Specification	17
5.4.1 Flow Models	17
5.4.2 Fluid Properties	17
5.5 Solving	19
5.5.1 Numerical Schemes	19
5.5.2 Solvers	19
5.6 Post-processing	21
5.7 Comparison with Other Programs	23
5.7.1 Maxsurf	23
5.7.2 Michlet	24
6.0 Results and Discussion	27
6.1 Restricted Channel Squat	27

6.2 Resistance	34
6.2.1 Deep Water	34
6.2.2 Shallow Water	43
6.3 Model Scale in Shallow Water	45
7.0 Conclusions and Recommendations	47
7.1 Conclusions	47
7.2 Recommendations	49
8.0 References	51
Appendix A: Equations	55
Appendix B: OpenFOAM files	57
Appendix C: Tables of Hydrostatics	63
Appendix D: Michlet Input File	66

List of Figures

Figure 5.1: Maxsurf Modeler Screenshot	8
Figure 5.2: Hull from underneath.....	9
Figure 5.3: Container ship in the stepped channel	10
Figure 5.4: Channel dimensions.....	10
Figure 5.5: Bow Mesh Figure 5.6: Stern Mesh.....	12
Figure 5.7: Refinement of free surface	13
Figure 5.8: Quality of mesh on hull surface.....	14
Figure 5.9: Cell normal's for y-axis Figure 5.10: Cell normal's for z-axis	14
Figure 5.11: Cell normal's for y-axis Figure 5.12: Cell normal's for z-axis	15
Figure 5.13: Water to air transition.....	18
Figure 5.14: Checking for Convergence	21
Figure 5.15: Body plan.....	22
Figure 5.16: Screenshot of Maxsurf Modeler	23
Figure 5.17: Screenshot of Michlet.....	24
Figure 5.18: Screenshot of Michlet resistance curve	25
Figure 6.1: Dynamic pressure OpenFOAM, T=14.0m, U=10kn	28
Figure 6.2: Seabed pressure Michlet, T=14.0m, U=10kn	29
Figure 6.3: Dynamic pressure OpenFOAM, T=14.0m, U=14kn	29
Figure 6.4: Seabed pressure Michlet, T=14.0m, U=14kn	30
Figure 6.5: Dynamic pressure OpenFOAM, T=14.5m, U=6kn	30
Figure 6.6: Seabed Pressure Michlet, T=14.5m, U=6kn.....	31
Figure 6.7: Dynamic pressure of ship and channel OpenFOAM, T=13.0m, U=10kn.....	32
Figure 6.8: Dynamic pressure of ship and channel OpenFOAM, T=14.5m, U=14kn.....	32
Figure 6.9: Channel fluid velocity (m/s) OpenFOAM, T=13.0m, U=10kn.....	33
Figure 6.10: Channel fluid velocity (m/s) OpenFOAM, T=14.5m, U=10kn.....	33
Figure 6.11: Channel elevation and wave pattern, T=14.5m, U=14kn.....	33
Figure 6.12: Actual channel geometry used in experiments	34
Figure 6.13: Free surface elevation and wave pattern OpenFOAM, T=14.5m, U=20kn	37
Figure 6.14: Free surface elevation and wave pattern Maxsurf, T=14.5m, U=20kn	37
Figure 6.15: Free surface elevation and wave pattern Michlet, T=14.5m, U=20kn	38
Figure 6.16: Free surface elevation and wave pattern OpenFOAM, T=14.5m, U=22kn	38
Figure 6.17: Free surface elevation and wave pattern Maxsurf, T=14.5m, U=22kn	39
Figure 6.18: Free surface elevation and wave pattern Michlet, T=14.5m, U=22kn	39
Figure 6.19: Free surface elevation and wave pattern OpenFOAM, T=14.5m, U=25kn	40
Figure 6.20: Free surface elevation and wave pattern Maxsurf, T=14.5m, U=25kn	40
Figure 6.21: Free surface elevation and wave pattern Michlet, T=14.5m, U=25kn	41
Figure 6.22: Free surface wave pattern and velocity magnitude, T=14.0m, U=10kn	41
Figure 6.23: Free surface wave pattern and velocity magnitude, T=14.0m, U=15kn	41
Figure 6.24: Shallow water dynamic pressure, T=14.0m, U=10kn	44

List of Tables

Table 5.1: Container Ship Dimensions	8
Table 5.2: Grid Sizes.....	11
Table 5.3: Channel boundary conditions	16
Table 5.4: Shallow water boundary conditions.....	16
Table 5.5: Deep water boundary conditions	16
Table 5.6: Model boundary conditions	17
Table 5.7: Fluid Properties.....	18
Table 5.8: Numerical Schemes	19
Table 6.1: Squat results in channel using OpenFOAM	27
Table 6.2: Experimental squat results in channel	28
Table 6.3: Deep water resistance OpenFOAM, T=14.0m	35
Table 6.4: Deep water resistance comparison, T=14.0m.....	35
Table 6.5: Deep water resistance OpenFOAM, T=14.5m	35
Table 6.6: Deep water resistance comparison, T=14.5m.....	35
Table 6.7: Deep water resistance coefficients OpenFOAM, T=14.5m.....	42
Table 6.8: Deep water resistance coefficients comparison, T=14.5m	43
Table 6.9: Shallow water resistance, T=14.0m.....	44
Table 6.10: Shallow water resistance, T=14.5m.....	44
Table 6.11: Model scale in shallow water OpenFOAM, T=0.35m.....	46
Table C.1: Table of offsets, T=14.0m.....	63
Table C.2: Simpson's rule, T=14.0m	64
Table C.3: Simpson's rule, T=0.35m	65

Nomenclature

A_{WP}	= waterplane area	m^2
BM_L	= longitudinal height difference between LCB and metacentre	m
C_B	= block coefficient	[-]
C_V	= viscous resistance coefficient	[-]
C_T	= total resistance coefficient	[-]
C_W	= wave resistance coefficient	[-]
C_{WP}	= waterplane area coefficient	[-]
C_S	= sinkage coefficient 2	[-]
C_θ	= trim coefficient 2	[-]
F_h	= depth based Froude number	[-]
F_B	= buoyancy force	N
F_Z	= downwards dynamic force	N
GM_L	= longitudinal height difference between LCG and metacentre	m
I_{LCF}	= second moment of waterplane area	m^4
L_{PP}	= length between perpendiculars	m
L_{WL}	= waterline length	M
M_y	= first moment of area	m^3
R_T	= total resistance	N
R_v	= viscous resistance	N
R_w	= wave resistance	N
V_{crit}	= critical speed	m/s
c_S	= sinkage coefficient	[-]
c_θ	= trim coefficient	[-]

k_m	= blockage correction coefficient	[-]
k_s	= ship dependant coefficient	[-]
\vec{n}	= point on hull surface	[-]
s_{LCF}	= sinkage at LCF	m
s_{max}	= maximum sinkage at midships	m
ν_T	= turbulent viscosity	m ² /s
θ_{max}	= maximum trim angle	radians
θ_w	= wave propagation direction	[-]
∇	= volume displacement	m ³
h	= undisturbed water depth	m
Φ	= velocity potential	m ² /s
B	= beam	m
$B(x)$	= waterline breadth at station x	m
K	= correlation coefficient for squat	s ² /m
LCB	= longitudinal centre of buoyancy	m
LCF	= longitudinal centre of floatation	m
M	= trimming moment	Nm
MTC	= moment to trim by 1cm	tonnes.m
Re	= Reynolds number	[-]
$S(x)$	= cross-section area at station x	m ²
SM	= Simpson's multiple	[-]
S_w	= wetted surface area	m ²
T	= draught	m
U	= velocity of fluid	m/s
V	= ship forward speed	m/s
W	= weight of the ship	N
$Y(x, z)$	= offsets	m
$Z(x, y)$	= free surface	m

g	= acceleration due to gravity	m/s^2
k	= turbulent kinetic energy	m^2/s^2
l	= length scalar	m
m	= mass of ship	kg
p	= pressure	Pa
p_{rgh}	= dynamic pressure	Pa
u	= velocity in x direction	m/s
u	= turbulent velocity	m/s
u'	= fluctuating velocity in x direction	m/s
v	= velocity in y direction	m/s
w	= velocity in z direction	m/s
x	= longitudinal coordinate	m
y	= transverse coordinate	m
z	= depth coordinate	m
i	= x vector component	$[-]$
j	= y vector component	$[-]$
k	= z vector component	$[-]$
Δ	= displacement of ship	kg
θ	= trim angle	radians
μ	= dynamic viscosity	Ns/m^2
ξ	= LCF of hull section forward or aft of parallel midbody	m
ρ	= water density	kg/m^3
σ	= normal stress	Pa
τ	= shear stress	Pa
ν	= kinematic viscosity	m^2/s
ω	= specific dissipation	$1/\text{s}$
ϕ	= flow perturbation	m^2/s

1.0 Introduction

1.1 Motivation for this Project

Examining the dynamics of a container ship is extremely important for designers of both the ship itself and the waterways in which they travel. For a large container ship a number of factors affect the operation, these include the overall length, beam, draught, shape of the hull, displacement, velocity and distribution of the weight and buoyancy. A restricted channel has influencing factors such as width, depth, geometry and underkeel clearance. All of these factors then affect the three main issues for a ship in shallow water; they are sinkage, trim and resistance. The original motivation for this project was from a workshop created at the University of Duisberg-Essen and Germanischer Lloyd to gather results for the dynamic squat of a particular container ship. The hull design used was the Duisburg Test Case which is a self propelled model (Moctar, Shigunov and Zorn 2012, 50). The workshop was designed to collect submissions that use various numerical methods and compare the results against the test case. Thus it was a perfect opportunity to do these simulations using the open source program on Linux called OpenFOAM.

Squat is the term used to describe both sinkage and trim at subcritical speeds (Tuck 1978, 33). It can be described as the loss of underkeel clearance (Barrass and Derrett 2012) due to dynamic pressure and motion of the ship. Ship squat is becoming an ever increasing problem with large bulk carriers and container ships when in restricted waters. With the world's population constantly growing, supply and demand is rising to a frightening level that could see this issue affect us even more in years to come. Ships are heavier, required to carry more and travel faster speeds to compensate for this. Squat is mainly affected by these parameters and so it is important to examine it and understand problematic areas. A container ship running aground will have massive implications and can affect various parties involved in the process. The process of moving the ship is costly, time wasting and can greatly affect the port schedule which has even further reaching problems such as loss

of profit. On top of this the ship and possibly the channel will need repairs and also there can be huge environmental issues.

The resistance of a ship is definitely not a new concept, however as mentioned before the changing environment of a container ships specifications requires there to be continual effort into improving resistance prediction methods. Resistance can affect the velocity of the ship which in turn requires more power and fuel. It can also cause damage to the hull and require repair work. It is clearly obvious how much of an expensive operation running and up keeping large container ships is becoming. Even though model testing of ships in towing tanks has been an excellent approach to determining resistance values (and sinkage and trim) up to now, with an increasing need for accuracy especially of wave resistance, a more sophisticated analysis is needed.

1.2 Objectives

The aim of this project was to determine the sinkage, trim and resistance of a container ship in a channel, shallow water and deep water. To calculate these values a computational fluid dynamics approach was used and the results were compared to two other boat design software's, Michlet and Maxsurf. One case from the workshop was provided so that the values obtained from the numerical analysis can be equated for accuracy. Two other benchmark testing's for the Duisburg Test Case vessel were also provided that required resistance values and coefficients, as well as sinkage and trim values. Therefore in order to achieve these results and discuss the validity of OpenFOAM, the objectives of the project were as follows.

1. For three varying cases in a restricted channel calculate the value of dynamic squat at the midships using OpenFOAM. The different cases were three draughts of 13.0, 14.0 and 14.5m and three speeds at 6, 10 and 14 knots.

2. For a model scale of the 14.0m draught ship in shallow water, calculate the wave and viscous resistance, trim and sinkage using OpenFOAM.
3. For draughts of 14.0 and 14.5m, calculate the wave and viscous resistance and their coefficients (only 14.5) in deep water using OpenFOAM. Compare these results with Maxsurf, Michlet and experimental.
4. Again for draughts of 14.0 and 14.5m, calculate the wave and viscous resistance in shallow water using OpenFOAM. Compare these results with those gathered from Michlet only.
5. Discuss the accuracy and appropriateness of OpenFOAM in calculating the squat, trim and resistance of a container ship in restricted channels, shallow water and deep water.
6. Recommend the areas of improvement and examine the opportunities and future prospects of CFD analysis in ship design, focusing on OpenFOAM.

1.3 Project Report Overview

As previously mentioned this chapter discusses the motivation behind the project and the objectives to be achieved. Thus the research and work carried out was broken down and divided into chapters that will be discussed here.

Chapter 2 reviews literature in all forms such as articles in journals, books, reports and thesis' and what these works have provided to the field of research in ship squat, trim and resistance. The chapter is in three sections including squat, resistance and CFD analysis on ships. The squat, sinkage and trim part has further topics discussed such as the slender body theory, GPS on full scale ships and comparison between empirical methods. The slender body theory is used by E. O. Tuck to create equations for sinkage and trim, based on

coefficients of sinkage and trim. The GPS methods involve placing receivers on ships and live recording their sinkage as they travel through a channel. Finally a quick examination of other squat formulae is done. Resistance is divided into the research done on wave and viscous resistances separately. The thin ship theory by J. H. Michell is introduced in the wave resistance section. The 1957 ITTC correlation line is discussed in viscous resistance. Finally the last section examines what CFD work has been done on ships mainly in the last 10 or so years.

Chapter 3 looks at the background theory of ship design and naval architecture. Basic principles such as buoyancy, hull definition and hydrodynamics have the theory and formulae provided in this section. Also more importantly the equations used in this work for calculating the trim and squat are listed in the hydrodynamics part. Other theory includes the block and waterplane area coefficients and Simpson's rule for calculating areas, volumes and second moments of area.

Chapter 4 discusses the theory of computation fluid dynamics. The process for setting up a CFD analysis, the governing equations of fluid dynamics such as the continuity, momentum and Navier-Stokes equations are all looked at. Also included is turbulence modeling in CFD, the Reynolds decomposition, Reynolds Average Stress (RAS) and the $k-\omega$ model.

Chapter 5 examines how CFD was approached in this project. Firstly the ship and channel geometry are outlined, with the dimensions for draughts of 13.0, 14.0 and 14.5m and also the stepped channel. Next the meshing is explained, about what was in the OpenFOAM dictionaries and utilities and how they worked. Also the quality of the mesh is observed by viewing figures of the grid underneath the hull, at the stern and bow and along the free surface. After this the boundary conditions for all the variables for each of the channel, shallow and deep water and model scale cases were listed. Flow specification discusses the

turbulent models and fluid properties used in the simulation. Then the numerical discretisation schemes for derivatives and interpolations were examined. The solver models like LTSInterFoam and Gauss-Seidel are then reviewed. It is then discussed what post-processing techniques are used to calculate the results needed. Lastly the method used for comparing the OpenFOAM results with the programs Maxsurf and Michlet.

Chapter 6 presents the results of the simulations run in OpenFOAM and discusses the errors and reasons for them. The first section is about the squat in the restricted channel and provides a table with values for squat at three draughts and speeds giving overall nine data points. Figures of the dynamic pressure for a number of different cases are also displayed. Part 2 of the results examines deep and shallow water resistance values. The total resistance is broken down into two components, wave and viscous. Adding to the discussion are figures of the wave patterns and elevations from OpenFOAM, Maxsurf and Michlet. Finally a model scale containership is used for determining sinkage, trim and resistance in shallow water and comparing to benchmark experimental data.

5.0 CFD Modeling Approach in this Project

The open source program OpenFOAM was used to model the geometry, mesh the structure, assign the boundary conditions, solve and post process the data obtained. In order to run a case in OpenFOAM the correct file structure must be used, otherwise errors will occur. All simulations that were run in this project had the same case file setup with just geometry and boundary conditions changing on each occasion. The first folder contained the initial and boundary conditions for each variable, hence it was called the zero time folder. Next was the constant folder which contained two pieces of information, the mesh and physical properties like acceleration due to gravity, viscosity and density. The mesh was defined by the geometry of the boundary and the geometry of the obstacle in this boundary (in this case the channel and ship respectively). Lastly was the system folder which contained all the necessities in order to solve the case, including numerical schemes, solvers, run parameters and the meshing procedure itself.

OpenFOAM on most occasions uses what are known as dictionaries which contain a set of instructions to follow. The dictionary is called by executing the command keyword for that particular dictionary. Each can contain subdictionaries which are used to divide the execution and provide a more structured simulation. They also have lists included that specify a set of coordinates, scalars or vectors. It is these dictionaries, the models and procedures used for the simulation that are outlined in this section of the report. The RANS equations outlined in the previous section are solved numerically using a finite volume method. The basic structure of each case was taken from the wigley hull example provided with the OpenFOAM package. The wigley hull is a simple shaped boat that is symmetrical and thin and used as a starting point for a lot of hydrostatic testing. Since it is a set hull that can be used for any program it is excellent to compare to other solution methods. From here the changes in geometry and mesh generation could be done to suit the cases in this project.

5.1 Geometry

5.1.1 Container Ship

The geometry of the ship was taken from the Duisburg Test Case container ship and its dimensions can also be obtained from (Moctar, Shigunov and Zorn 2012, 50). This benchmark paper only has the dimensions for the ship when the draught is 14.5m. The simulations that were carried out in this project include draughts of 13.0, 14.0 and 14.5m. On each occasion the overall length and beam of the container ship stays the same. While the waterline length, waterplane area and wetted surface area change accordingly. To determine these values a software program called Maxsurf was utilised. The particular suite of this software is the Modeler program, and this can import a range of files. The ship geometry was obtained as an IGES file which maps out all of the surfaces.

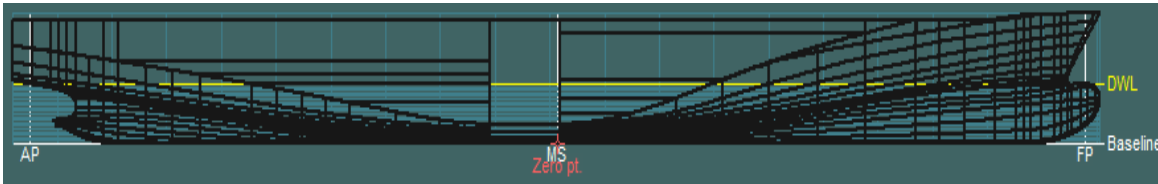


Figure 5.1: Maxsurf Modeler Screenshot

Thus according to this procedure the following table provides the results for all three draughts.

Table 5.1: Container Ship Dimensions

T (m)	L_{WL} (m)	B (m)	A_{WP} (m ²)	S_W (m ²)	∇ (m ³)
13.0	355.87	51.0	14748.95	19769.37	151152.06
14.0	360.79	51.0	15223.61	20782.13	166124.14
14.5	361.82	51.0	15473.56	21323.92	173815.65

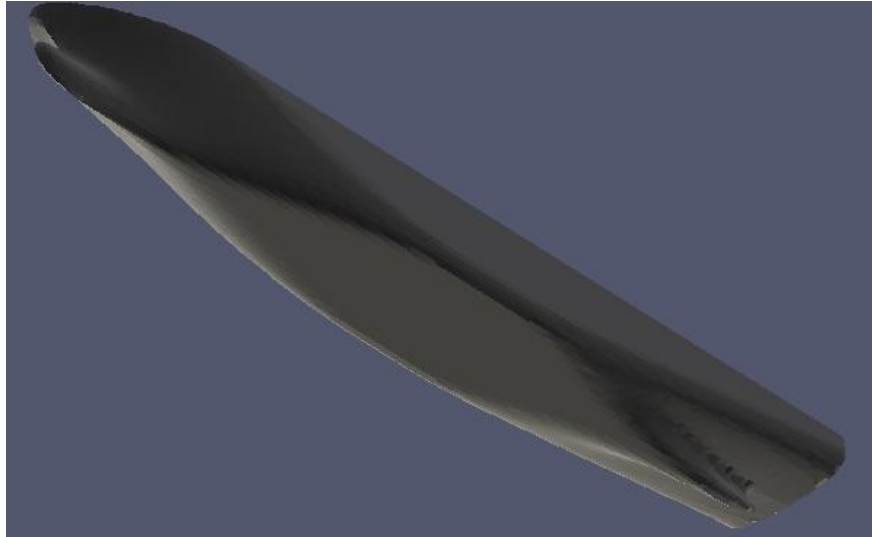


Figure 5.2: Hull from underneath

5.1.2 Channel

There were three different boundary geometries used with this ship, they included a stepped channel, shallow water and deep water. The shallow water cases used the same depth as the stepped channels however the sides were positioned far enough away from the ship so that they did not affect the solution, thus creating open water. The dimensions for this included the inlet at 560m forward of the midships and the outlet 932m aft of the midships, 500m either side in the y-direction and a depth of 16m. The deep water dimensions set out to achieve the same as the shallow water, by doing the tests in open water so as to not conflict with results. These dimensions were inlet at 500m forward, outlet at 1000m aft, 500m either side and a depth of 500m.

The dimensions for the channel were taken from the workshop at the University of Duisberg-Essen (Pre Squat 2013). One slight change was made to the channel which has the sides of the channel on an angle. Since this was difficult to model in OpenFOAM the sides were changed to be stepped however keeping the same horizontal dimension in the y-direction. Figures 5.3 and 5.4 show the ship and channel set up and the channel dimensions respectively. The inlet is 560m forward and the outlet is 932m aft of the midships.

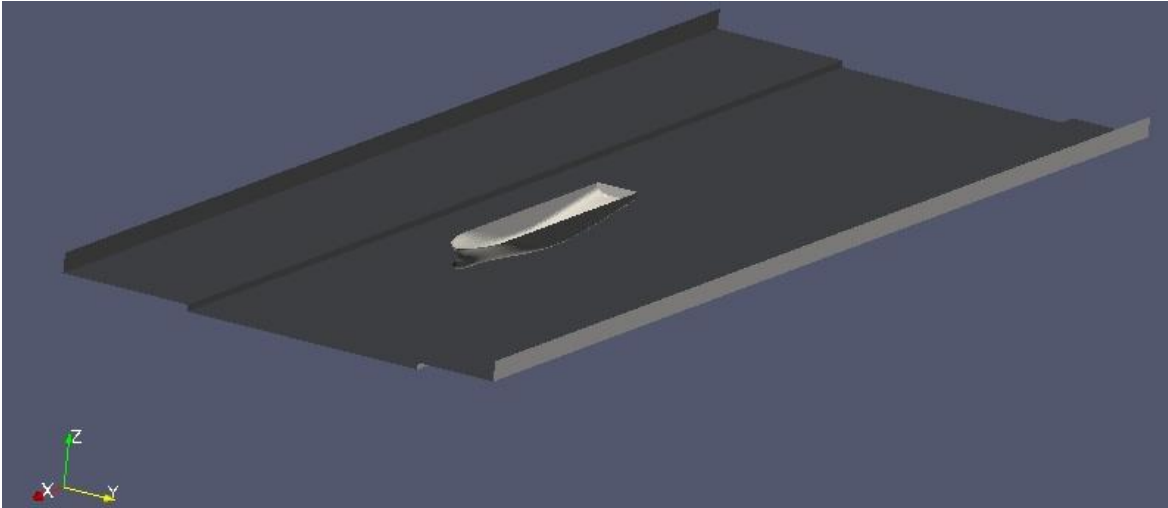


Figure 5.3: Container ship in the stepped channel

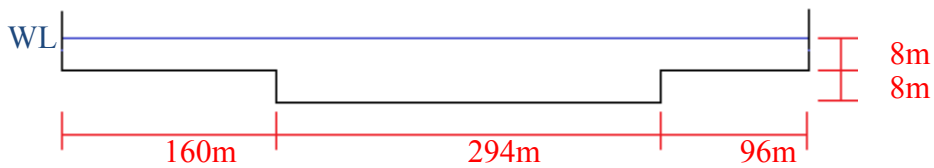


Figure 5.4: Channel dimensions

5.1.3 Model Scale

In an effort to compare full scale simulations with model scale and also numerical against experimental model scale testing, a scaled down geometry was developed. The benchmark paper (Moctar, Shigunov and Zorn 2012, 50) used a scale of 1:59.407 of the 14.5m draught for their experiments, however this project used full scale in the simulations.

Also an alternative benchmark was provided which had the 14.0m draft ship scaled down 1:40. The width of the tank was 10m and the depth was 0.4m. This time however OpenFOAM used the scaled down dimensions of the ship and tank. This was achieved by importing the STL file created from the IGES file into another program called Blender and the boundary dimensions were adjusted to suit. These dimensions gave a shallow water case much like before however it is not in open water, as the side dimensions may affect the results.

5.2 Grid Generation and Meshing

The two most important files used in OpenFOAM to create the mesh are the `blockMeshDict` and the `snappyHexMeshDict`. The first is situated in the `constant` folder and the other is in the `system` folder of the case folder structure mentioned at the start of this chapter. The `blockMeshDict` creates by namesake 3D meshes that are blocks or cubes. An example for the channel is in Appendix B. The mesh that is generated contains equal sized cells throughout that make up the discretised grid. The shallow and deep water cases are simple to create because they are just one block, however the channel is created by combining four blocks. These are obvious to see if Figure 5.4 is examined, by ignoring the waterline three blocks make up the top part and the last is the 8 by 294m section on the bottom. The dictionary first lists the vertices that make up the dimensions mentioned in section 5.1.2. Next these points are used to distinguish the 8 vertices for each block, as well as the number of cells in each the x, y and z directions. Lastly the boundary patches or symmetry planes are specified using the vertices. Each of these boundaries is what is used to specify the conditions of the simulation. They include inlet, outlet, sides of the channel and the atmosphere. The number of points, cells and faces created by each `blockMesh` for the channel, shallow water, deep water and model cases are listed in the table below.

Table 5.2: Grid Sizes

	Channel	Shallow	Deep	Model
Points	420002	464121	12268880	464121
Cells	364048	408480	12093750	408480
Faces	1147578	1280564	36455625	1280564

The `snappyHexMeshDict` is used to mesh an obstacle internally into the `blockMesh` created previously. The container ship here is the obstacle and must be in STL form so that the surfaces are recognised. This utility is very useful to create a new patch that is the surface of the hull. A few subdictionaries are used throughout the script, however to start with the `trisurface` mesh of the ship that has already been created must be specified and in effect

imported. The cells are completely hexes and must be split into parts where they intersect with the hull. Upon splitting the cells they are then refined at the surface. This is done by specifying a minimum level to applied across the entire surface and a maximum level that can be applied to those cells that are not so simple (OpenFOAM 2011). For most cases in this project the minimum and maximum levels were both 1. Figures 5.5 and 5.6 show the mesh underneath the hull to be fair, with each cell having good size and shape.

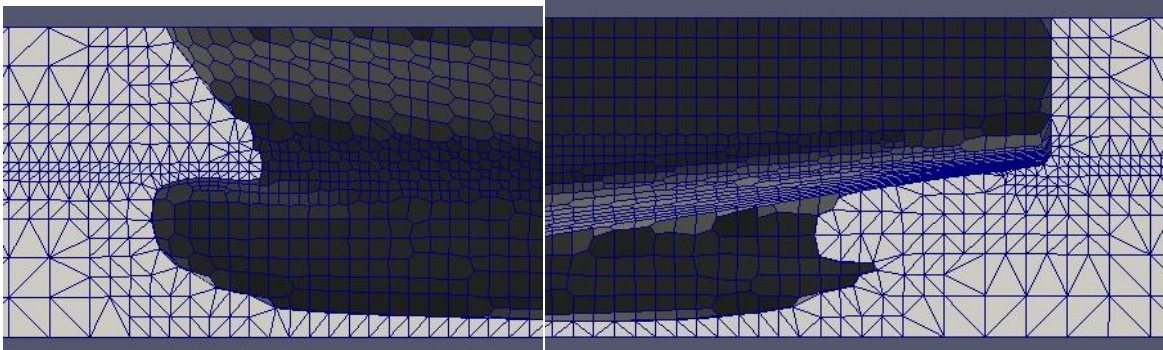


Figure 5.5: Bow Mesh

Figure 5.6: Stern Mesh

All the cells inside the hull wall are then removed, and more refinement is done in other areas. The main region that is refined for all cases is the free surface, or the interface between the air and water. This is possibly the most important because of how these two fluids react due to the difference in their properties. For all cases small regions above and below this surface are refined to a minimum level of 1 and maximum of 2.

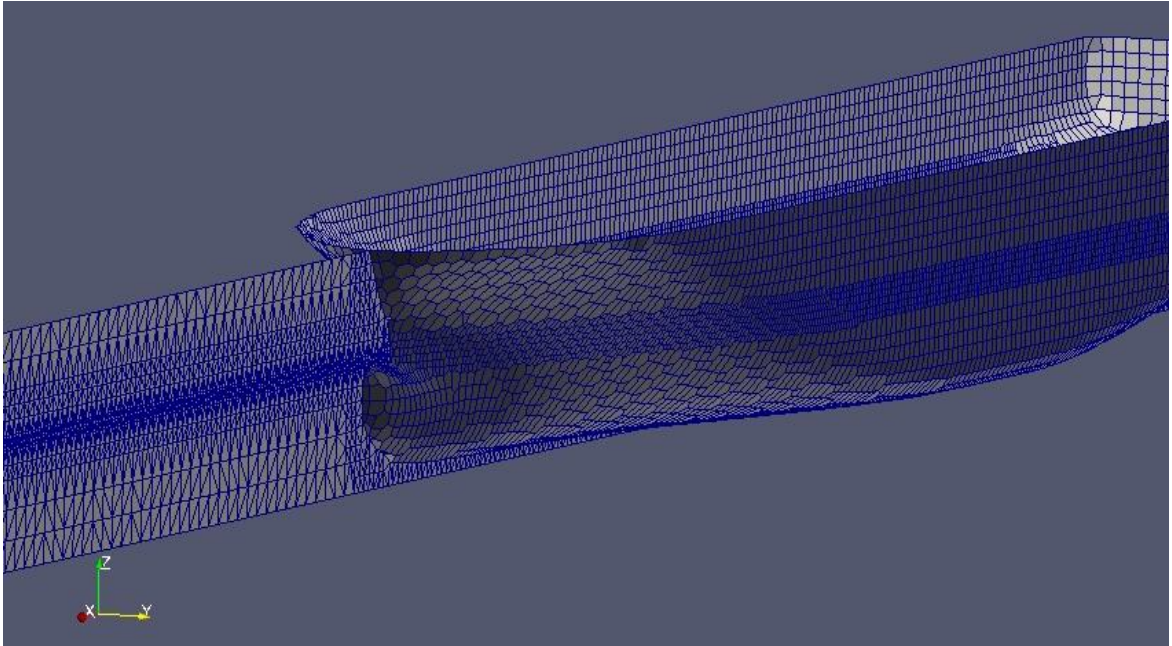


Figure 5.7: Refinement of free surface

There may still be small bits of cells left inside the hull and snapping is one way that these are removed. The surface is effectively smoothed so there are no sharp edges. Throughout this entire process there are mesh quality controls by which the meshing and snapping follows. If the cells are still outside the unwanted quality region then they are continued to be refined. Some controls for all cases included a max non-orthogonal angle of 65° , maximum skewness at the boundary of 20 and internally of 4. The quality can be based on the aspect ratio, and this should be as close to 1 as possible. Figure 5.8 shows this and most of the cells have a quality close to 1. Although the areas at the bow and stern are closer to 0, therefore they are not as high quality.

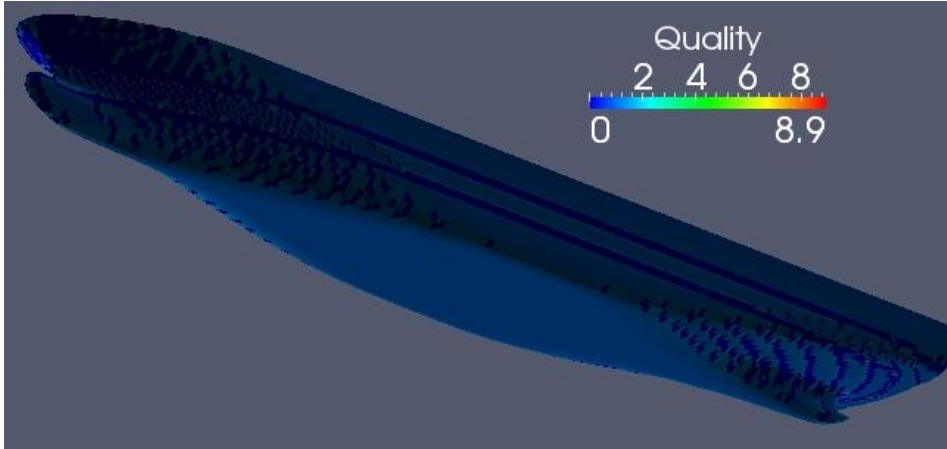


Figure 5.8: Quality of mesh on hull surface

Finally the smoothness of transition between the cell faces at the bow and stern can be observed in the following figures. These pictures show how orthogonal the cell face is to the y and z axis. The gradient of change in colour should flow nicely between cell boundaries. However it can be noticed that the larger the cells are the less achievable this is. The worst sections are around the bulb and rudder. Thus it would have been good to do refinement at these spots as well.

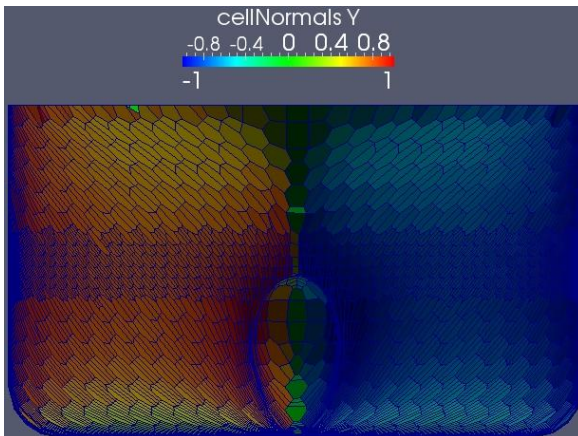


Figure 5.9: Cell normal's for y-axis

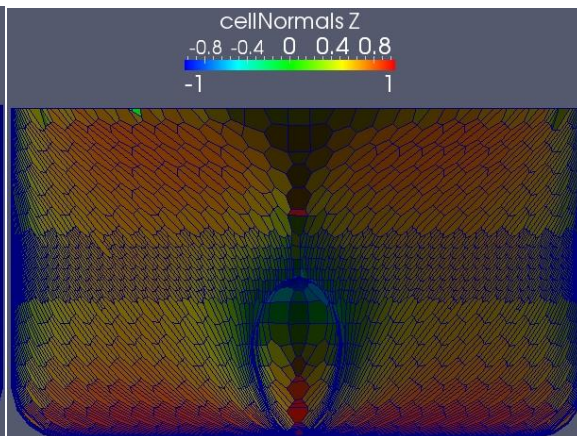


Figure 5.10: Cell normal's for z-axis

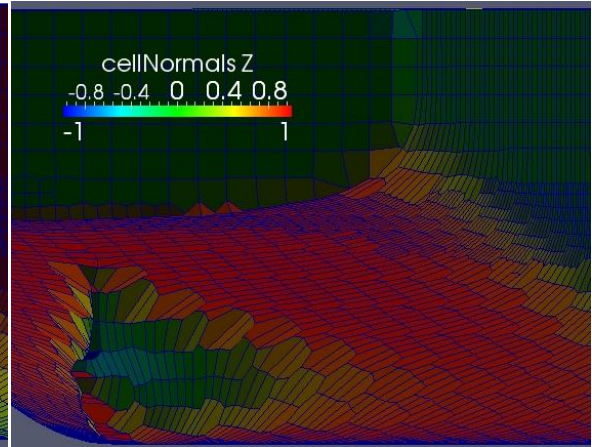
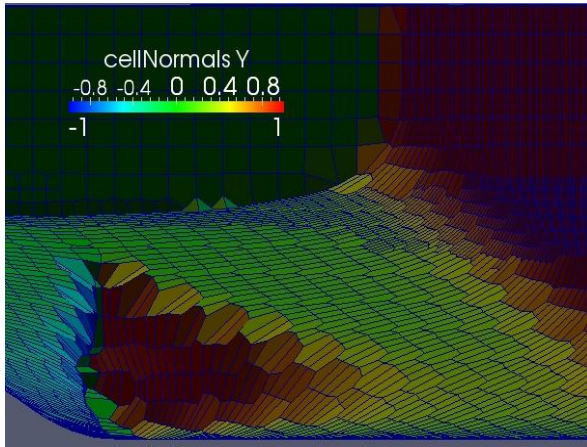


Figure 5.11: Cell normal's for y-axis

Figure 5.12: Cell normal's for z-axis

5.3 Initial and Boundary Conditions

The initial and boundary conditions are situated in the zero time folder as mentioned before in the case folder structure. For each variable the condition is given for all the patches created by the blockMesh and the addition of the hull wall from the snappyHexMesh. The tables below give the boundary conditions for each variable and for each type of case. Some annotations are as follows, SP is symmetry plane, FV is fixed value, BP is buoyant pressure, ZG is zero gradient, TP is total pressure, WF is wall function, PIOV is pressureInletOutletVelocity and IO is inletOutlet. The numbers in the brackets are the uniform value assigned for the field at that boundary.

For most boundaries they have the type patch which means it doesn't have geometric information for the mesh. The hull is a wall type which allows wall functions to be assigned for the turbulence model and others are symmetry plane which means that values on both sides of the plane are equal. Zero gradient means that the field at that boundary has a zero normal gradient. Buoyant pressure is the same as zero gradient however it is specifying it for dynamic pressure. InletOutlet means the flow is mixed depending on the direction of the velocity. When the flow is in then the value is fixed and when it is out the value is zero gradient. Total pressure is assuring that the addition of hydrostatic and dynamic pressure is fixed. Hence it is a balance between the pressure and velocity. PressureInletOutletVelocity

is combination of inletOutlet and changing pressure and velocity. The only value that is changed between cases of the same geometry is the velocity.

Table 5.3: Channel boundary conditions

Boundary	Type	U	p_rgh	$alpha$	k	nut	ω
Inlet	patch	FV (5.14)	BP (0)	Calc (0)	FV (0.00015)	FV (5e-07)	FV (2)
Outlet	patch	ZG	BP (0)	ZG	ZG	ZG	ZG
Sides	patch	FV (5.14)	BP (0)	ZG	ZG	ZG	ZG
Atmosphere	patch	FV (5.14)	TP (0)	IO	IO	ZG	IO
Hull Wall	wall	FV (0)	BP (0)	ZG	kqR WF	Nutk WF	ω WF

Table 5.4: Shallow water boundary conditions

Boundary	Type	U	p_rgh	$alpha$	k	nut	ω
Inlet	patch	FV (5.14)	BP (0)	Calc (0)	FV (0.00015)	FV (5e-07)	FV (2)
Outlet	patch	ZG	BP (0)	ZG	ZG	ZG	ZG
Sides	SP	SP	SP	SP	SP	SP	SP
Atmosphere	patch	FV (5.14)	TP (0)	IO	IO	ZG	IO
Hull Wall	wall	FV (0)	BP (0)	ZG	kqR WF	Nutk WF	ω WF

Table 5.5: Deep water boundary conditions

Boundary	Type	U	p_rgh	$alpha$	k	nut	ω
Inlet (0 or 1)	patch	FV (5.14)	BP (0)	FV (0 or 1)	FV (0.00015)	FV (5e-07)	FV (2)
Outlet (0 or 1)	patch	ZG	BP (0)	ZG	ZG	ZG	ZG
Sides	SP	SP	SP	SP	SP	SP	SP
Atmosphere	patch	PIOV (0)	TP (0)	IO	IO	ZG	IO
Hull Wall	wall	FV (0)	BP (0)	ZG	kqR WF	Nutk WF	ω WF

Table 5.6: Model boundary conditions

Boundary	Type	U	p_{rgh}	$alpha$	k	nut	ω
Inlet	patch	FV (0.791)	BP (0)	Calc (0)	FV (0.00015)	FV (5e-07)	FV (2)
Outlet	patch	ZG	BP (0)	ZG	ZG	ZG	ZG
Sides	patch	FV (0.791)	BP (0)	ZG	ZG	ZG	ZG
Atmosphere	patch	FV (0.791)	TP (0)	IO	IO	ZG	IO
Hull Wall	wall	FV (0)	BP (0)	ZG	kqR WF	Nutk WF	ω WF

5.4 Flow Specification

5.4.1 Flow Models

To help solve the RANS equations a turbulent model must be selected. The simulation model used in this project was the Reynolds Average Stress (RAS) model. And the RAS model utilises the k - ω Shear Stress Transport (SST) turbulence model. These turbulence parameters have values according to the initial conditions provided in the previous section. It also allows for the use of the different wall functions at boundaries in turbulent fields k , q , R and ω . This model was chosen because it performs well in regions where separation occurs in the flow. This is a characteristic of hydrodynamics that is why it is mostly used for this type of modeling (Zhang 2010, 932).

5.4.2 Fluid Properties

The free surface is where the interaction between air and water is, and can often become unstable. Therefore an appropriate technique needs to be used to make sure it models this section correctly. Since this a multiphase situation the best approach is the coupled volume of fluid (VOF) method. This is an excellent way of modeling ships that produce breaking waves, because it can be used for two immiscible fluids where the interface position of these fluids is required to be calculated throughout the simulation (Zhang, Liu, et al. 2006, 315). The volume fraction is used to calculate the value of $alpha$. For values of 0 the fluid is air and for values of 1 the fluid is water. Anything between this is a mixture of the two and hence there will be an interface. The continuity equation for $alpha$ is used to locate the

interface by determining where alpha is changing at the fastest rate (Zhang, Liu, et al. 2006, 315).

For some cases like in deep water it was best to split the alpha into either equaling 0 or 1. There was only one value in between this that a cell could have and that was 0.5. This meant there was no gradual change in fluid like in Figure 5.13, it just changed instantaneously. The utility setFields was used to calculate the values of alpha by specifying a box that is all of a value 1, everything else was 0. Table 5.7 also has the fluid properties as specified in the dictionary transportProperties.

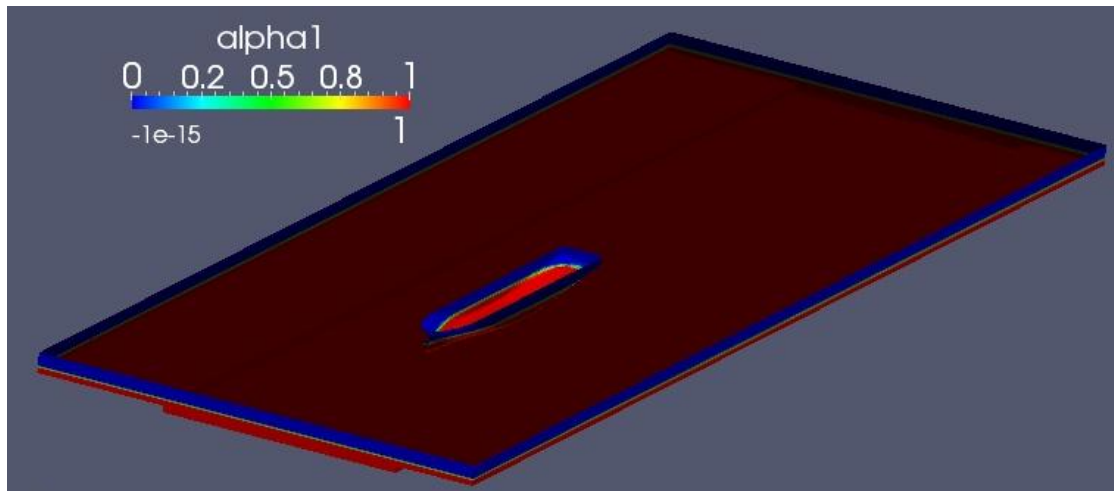


Figure 5.13: Water to air transition

Table 5.7: Fluid Properties

Fluid	ν	ρ
Air	1.48e-05	1.0
Water	1.0e-06	1000

5.5 Solving

5.5.1 Numerical Schemes

In the system directory the fvSchemes dictionary, where fv stands for finite volume method, is used to set out what numerical schemes are used for the simulation. Subdictionaries contain terms that include derivatives and interpolations that require numerical schemes in order to discretise the RANS and other equations. These subdictionary schemes include time, gradient, divergence (convection), laplacian, interpolation, components of gradient that are normal to the cell face and flux. Gaussian integration is used for most which works by interpolating from the cell centre to the cell face and then adding all of these together (OpenFOAM 2011). The following table lists the schemes assigned to each, where default means it has been applied to all variables. Only the convection term is mentioned for divergence, the others can be seen in Appendix B.

Table 5.8: Numerical Schemes

Term	Variable	Scheme	Description
Time	default	localEuler	Local time step, first order, bounded, implicit
Gradient	default	Gauss linear	Second order, linear interpolation
Divergence	Div(rho*phi, U)	Gauss linear upwind	Second order, linear interpolation, upwind differencing
Laplacian	default	Gauss linear corrected	Second order, linear interpolation, unbounded and conservative
Interpolation	default	linear	Linear interpolation
snGradient	default	corrected	Explicit non-orthogonal correction
Flux	p_rgh, pcorr, alpha1	-	Flux generated for these fields

5.5.2 Solvers

Again situated in the system directory of the case folder, fvSolver is the dictionary that specifies how the equations are solved after the numerical schemes have discretised the domain. The first subdictionary lists the solvers used for each of the variables. All use

Gauss-Seidel as the smoother, pcorr and p_rgh use generalized geometric-algebraic multi-grid (GAMG) as the solver and the rest use smoothSolver. The tolerances for each variable are also listed, so as to calculate the residual after each iteration. The pressure implicit split operator (PISO) algorithm is used for solving the pressure and velocity equations. It works by calculating an initial value and then using up to four corrections to get a final solution.

The solver used was LTSInterFoam which is what was typed into the command line to execute the simulation. This uses local time stepping to solve for two incompressible, isothermal and immiscible fluids (OpenFOAM 2011). This is how the multiphase situation is set up and solved. The simulations required a large amount of time and computer memory to complete. Therefore they were run in parallel using mpirun on iVEC's Epic system, where anywhere between 1 and 6 nodes were used. Each node had 12 cores with 24GB of RAM available. The channel cases would take roughly 300 CPU hours and the deep cases 650 CPU hours.

5.6 Post-processing

Firstly it was required to see if the simulation had converged, this was done by examining the residuals of the dynamic pressure. For each time step a residual is given, therefore these values can be plotted on a graph. The following graph displays it for one of the deep cases and it clearly shows convergence is achieved.

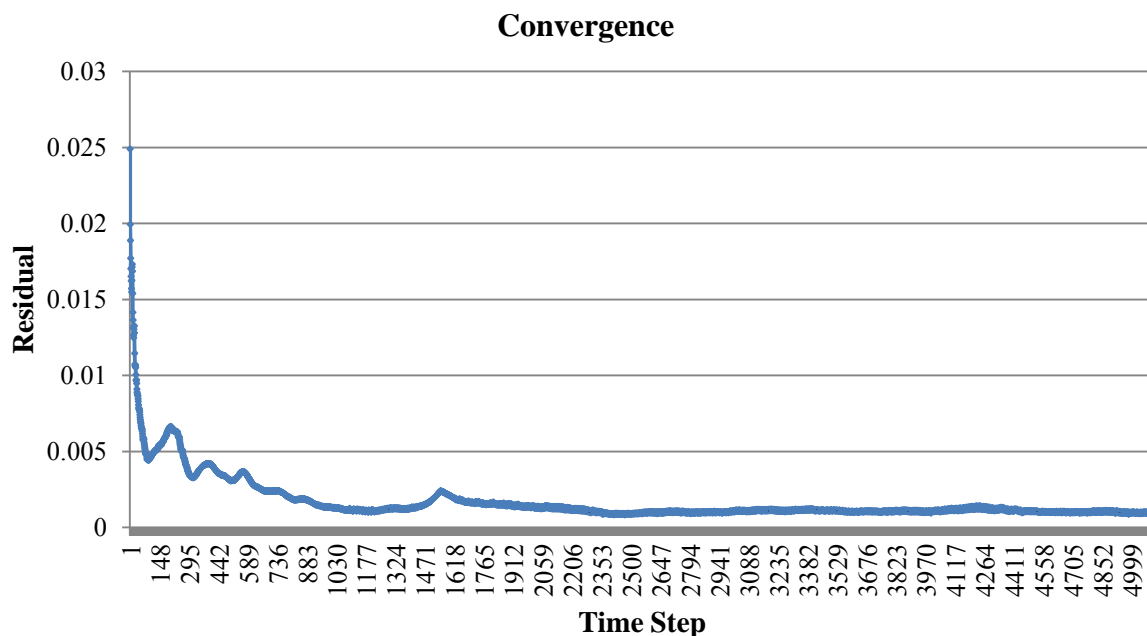


Figure 5.14: Checking for Convergence

The values calculated are only for those that were given initial conditions including pressure, dynamic pressure, velocity and alpha. For all of the calculations in this project the forces and moments acting on the hull are required. In order to do this both pressures were integrated over the entire area of the patch known as hull wall, since force equals pressure multiplied by area. This gave the forces and moments broken down into pressure force (wave) and viscous. These were further divided into the x, y and z components. Then equations 3.7 to 3.12 could be used to determine all the appropriate values that were being analysed. Maxsurf was again used as an aid to obtain the table of offsets. This was done by dividing the hull into 21 stations along the waterline length and 21 waterlines over the

submerged section of the hull. The position of the stations on the hull is shown in the Figure 5.15. Using Simpson's rule and the table of offsets further values could be determined for instance the second moment of area about LCF. An example of these tables for a draught of 14.0m is in Appendix C.

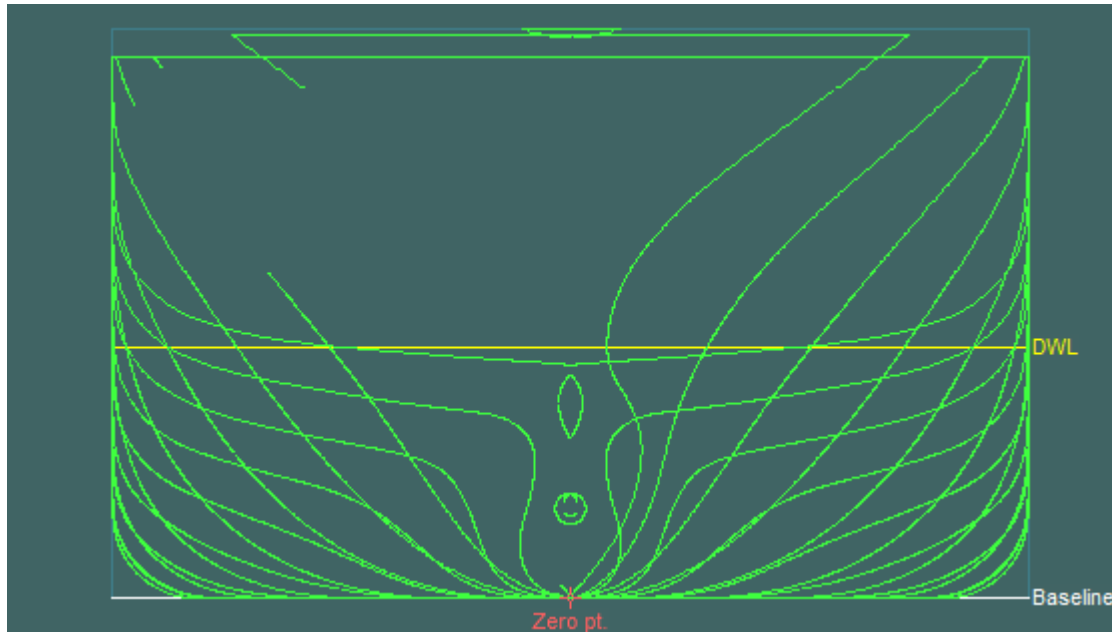


Figure 5.15: Body plan

Paraview was the program used to obtain visual results of the pressure, velocity and alpha distribution on the hull surface. The hull could be singled out and a graphic of the dynamic pressure changing over the surface was the most important. It was also used to show the grid and mesh of the entire system. Large quantities of data again hindered the use on a regular computer, so some functions were done on the supercomputer. With the use of the utility sampleDict the hull by itself, an isosurface of the free surface and a plane through the origin in the direction of the x-axis could all be obtained. These individual files were then viewed in Paraview and further figures were made.

5.7 Comparison with Other Programs

In order to gauge how accurate the results from OpenFOAM are they need to be compared with other methods. Experimental values in testing tanks are already provided by benchmark papers, however not many values are given. Therefore to somewhat validate the CFD analysis two other programs have been utilised to do so, these are Maxsurf and Michlet. Both could calculate the wave and viscous resistance, however Maxsurf could only do it in deep water. They could also determine the free surface wave plots. Neither could calculate the sinkage or trim.

5.7.1 Maxsurf

Maxsurf is naval architecture software that can model all sorts of hull forms. Some of the features include setting up a frame of reference with draught, design grid, calculating hydrostatic values, determining offsets, calculating resistance with many methods and free surface. The program was able to import the IGES file of the container ship into Maxsurf Modeler. From here the draught was added and also the sections, waterlines and buttocks. The offset for each station was determined individually and then combined to make the complete table (Appendix C). The design was then saved and opened in another branch of Maxsurf to calculate the resistance.

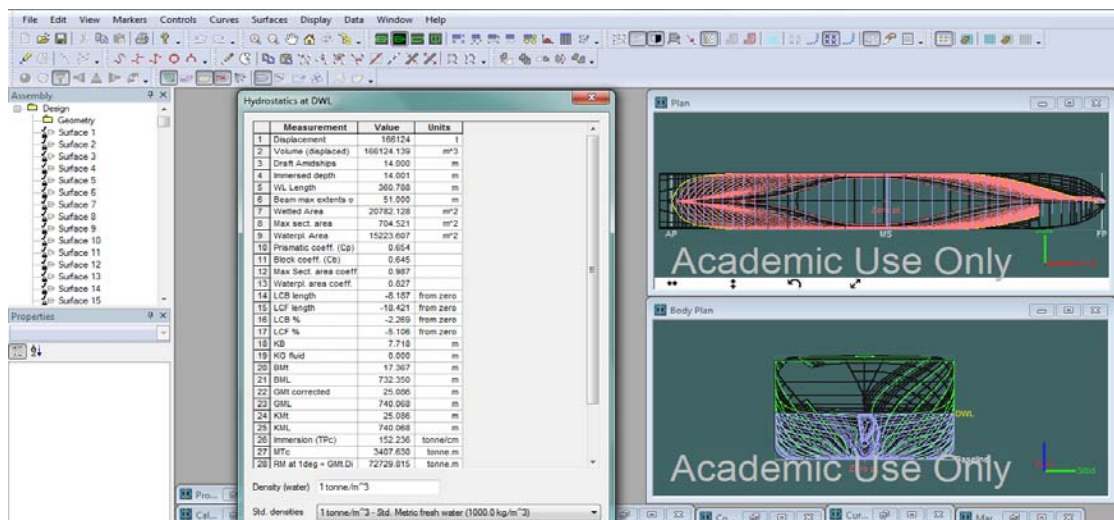


Figure 5.16: Screenshot of Maxsurf Modeler

Various methods for planning and displacement hulls could be used for calculating the resistance. These methods are based on many experiments and empirical equations were formed. The methods chosen for this project were the Slender Body Theory and the 1957 ITTC friction line. The hull data is inputted and these methods provide curves for the total resistance and coefficients of total, wave and viscous resistance against speed. It is just a matter of reading of the graph for at a particular speed. All three draughts were analysed however only in deep water. The free surface was also plotted in this same program.

5.7.2 Michlet

Michlet is a great program that is simple to use and gives effective results. All that is needed is the table of offsets in excel.csv format and an MLT file which can be opened and modified in Notepad on Windows. The input file specifies all the information that is required for modeling the hull. More than one hull can be modeled at once so that interference between the two can be observed. An example of the input file is provided in Appendix D. Firstly the physical properties of water and air are listed. Then the calculation parameters are chosen, the ITTC 1957 or Grigson friction methods, Slender Body Theory for pressure signature method and a form factor. Lastly the hull geometry is to be provided, this includes a reference to the offsets, displacement, waterline length and beam. The interface that appears when the program is executed is given below.

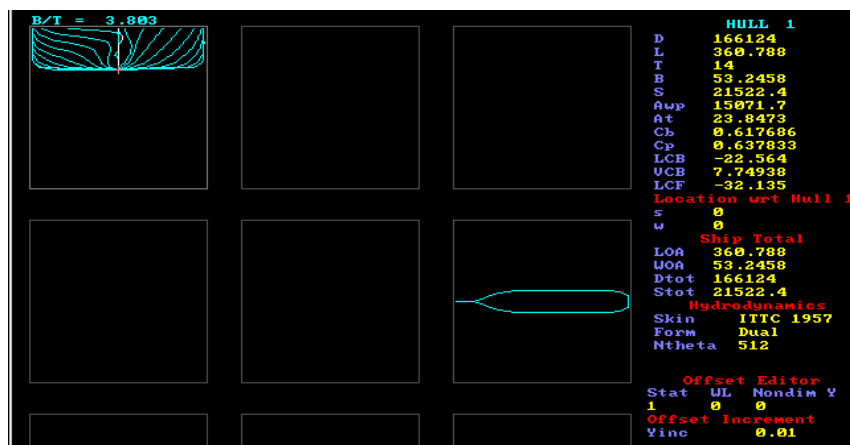


Figure 5.17: Screenshot of Michlet

It is first noticed that some of the hydrostatics are calculated including waterplane area, wetted surface area, form coefficients, LCB and LCF. Also the plan view of just the waterline and body plan showing all the stations. From this central part of the program the user can choose to view the resistance or pressure results, or plot the free surface wave pattern. The resistance gives a curve like the one below with all types of resistance provided. Both shallow and deep water resistance values were calculated.

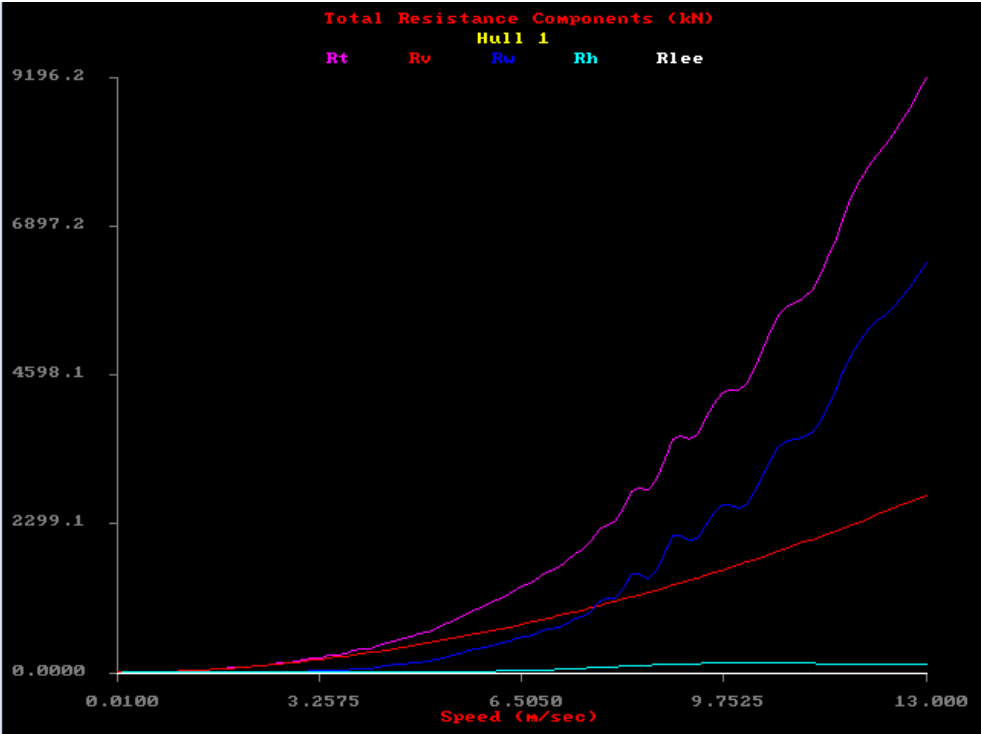


Figure 5.18: Screenshot of Michlet resistance curve

6.0 Results and Discussion

According to the objectives in chapter 1 the results reflect the outcomes of simulations for the container ship in a restricted channel, shallow and deep water. For these cases some provide the squat (sinkage and trim) and others the wave and viscous resistance. The values obtained from OpenFOAM are the most important, hence it is these that will be discussed in most detail. The experimental data and other programs provide results only as a means of comparison to determine the accuracy of OpenFOAM in predicting hydrodynamic terms. Figures are not provided for every result, only those that backup the discussion. The processes and numerical techniques for the CFD analysis have all been outlined in the previous chapter, therefore only the raw data is presented and an examination of these follows.

6.1 Restricted Channel Squat

Post-processing the dynamic pressure values from OpenFOAM gave the change in buoyancy force between the static and dynamic conditions. They were then used in equation 3.12 as the force in the z-direction. The waterplane area was also taken from Table 5.1, hence the values for squat for a number of cases are provided below. Table 6.2 displays the experimental data taken from the PreSquat workshop (Pre Squat 2013).

Table 6.1: Squat results in channel using OpenFOAM

Speed (kn)	Draught (m)		
	14.5	14.0	13.0
6	0.470	0.305	0.171
10	0.908	0.727	0.576
14	1.558	1.277	1.273

Table 6.2: Experimental squat results in channel

T=14.5m		T=14.0m		T=13.0m	
Speed (kn)	Squat (m)	Speed (kn)	Squat (m)	Speed (kn)	Squat (m)
6.35	0.23	6.81	0.22	5.07	0.065
9.79	0.585	10.04	0.585	10.58	0.55
12.21	1.06	13.25	1.33	13.59	1.345

The following figures of the hull illustrate how the negative dynamic pressure in effect pulls the hull closer to the channel seabed. It is also noticed that the data point for a draught of 13.0m at 10knobs obtained by OpenFOAM is about 5% higher than the experimental value which is quite good. All other values are considerably larger in OpenFOAM except for the draught at 13.0 and 14.0m and higher speeds which are smaller. The observation of OpenFOAM determining generally larger values can be validated by comparing the dynamic pressure values to Michlet which calculates the seabed pressure.

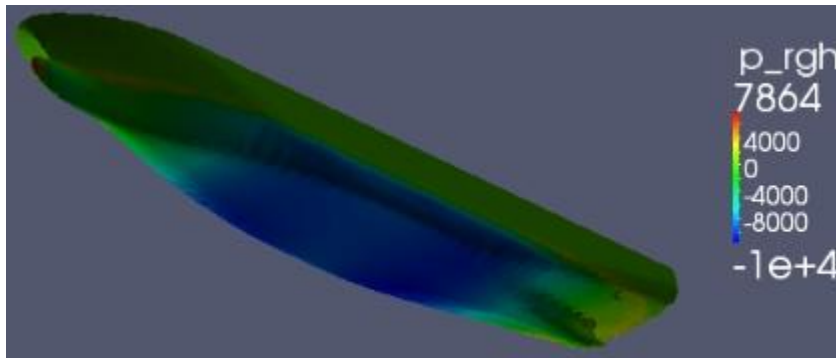


Figure 6.1: Dynamic pressure OpenFOAM, $T=14.0m$, $U=10kn$

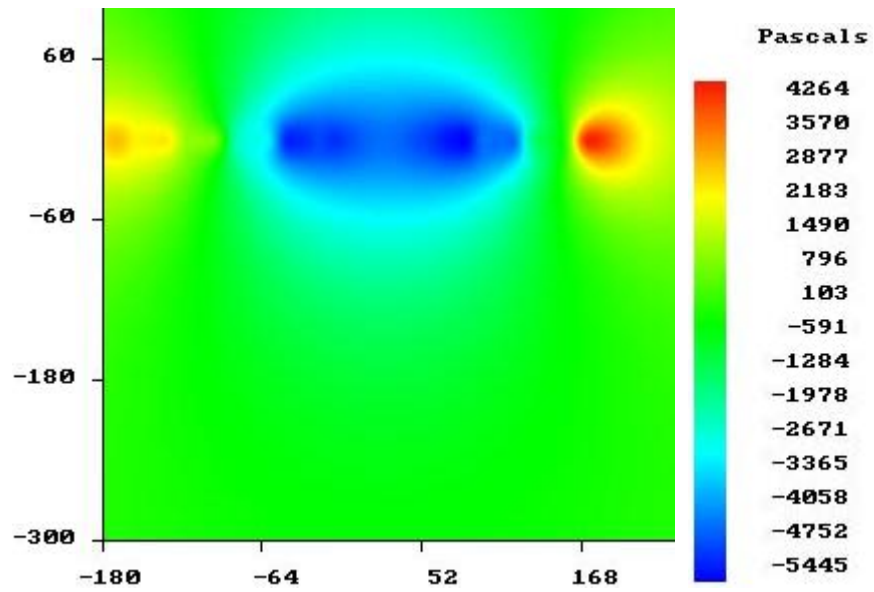


Figure 6.2: Seabed pressure Michlet, $T=14.0m$, $U=10kn$

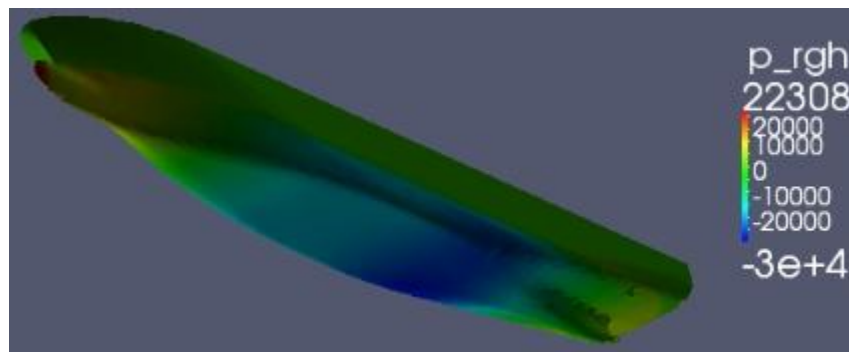


Figure 6.3: Dynamic pressure OpenFOAM, $T=14.0m$, $U=14kn$

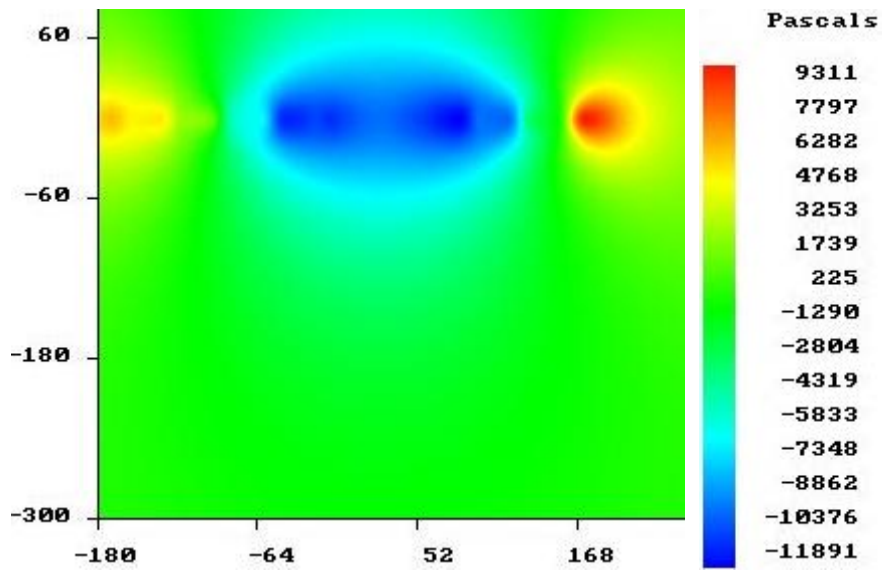


Figure 6.4: Seabed pressure Michlet, $T=14.0m$, $U=14kn$

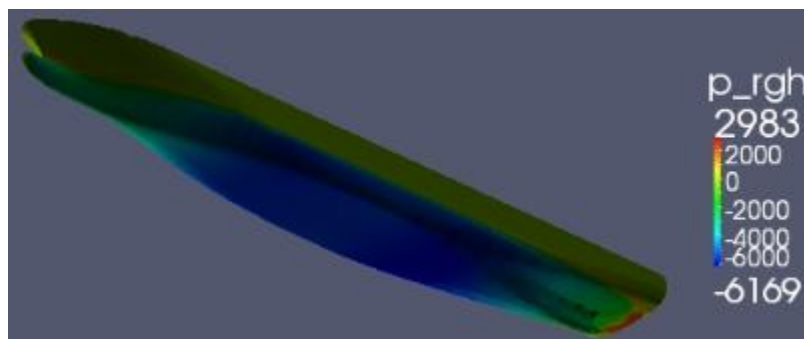


Figure 6.5: Dynamic pressure OpenFOAM, $T=14.5m$, $U=6kn$

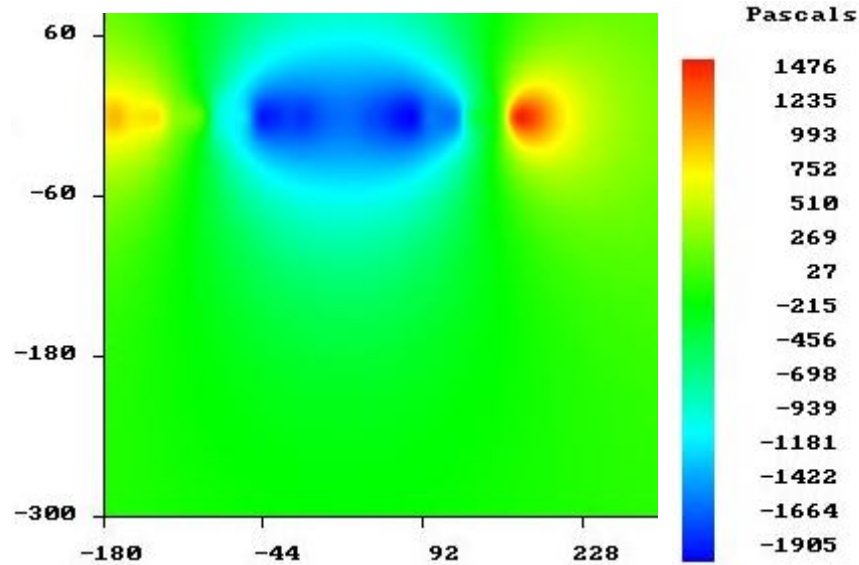


Figure 6.6: Seabed Pressure Michlet, $T=14.5m$, $U=6kn$

It is clearly noticeable that OpenFOAM calculates a larger pressure value in all cases. This will lead to a larger force on the hull and hence a larger squat value. Although Michlet cannot be considered to be completely accurate itself, the pattern between it and the experimental data does provide further backup to this conclusion.

The results show that as the velocity and draught increases the squat also increases. This confirms the theory that squat is directly proportional to the velocity. In fact the result of the 14.5m draught at 14knots shows that the ship will be hitting the seabed, because the depth of the channel is only 16.0m. This just proves how important it is to calculate the squat for such large container ships. Figures 6.9 and 6.10 demonstrate how the velocity of the water increases dramatically as it flows underneath the hull. For a good understanding of the severity, 10knots equals 5.14m/s. Figures 6.7 and 6.8 display that there is little difference in pressure value between the hull surface and the seabed, further validating the appropriateness of using Michlet as a comparison.

What is of great interest is that the highest positive pressure on the bottom surface of the hull occurs at the stern and therefore the squat will be greatest at the stern. This is true even though the bulb at the bow has high pressure it is not completely underneath. Also the greatest negative pressure seems to be aft of the midships which is best illustrated in Figures 6.3 and 6.8. Therefore the positive pressure could be a reaction to this or could be due to the velocity of the water having a magnitude of 0m/s at the stern as seen in Figures 6.9 and 6.10. The wave pattern and elevation of the free surface for the ship in the channel is also shown. Most notably no clear wave pattern forms only near field waves occur, so the free surface is random in nature.



Figure 6.7: Dynamic pressure of ship and channel OpenFOAM, $T=13.0m$, $U=10kn$



Figure 6.8: Dynamic pressure of ship and channel OpenFOAM, $T=14.5m$, $U=14kn$

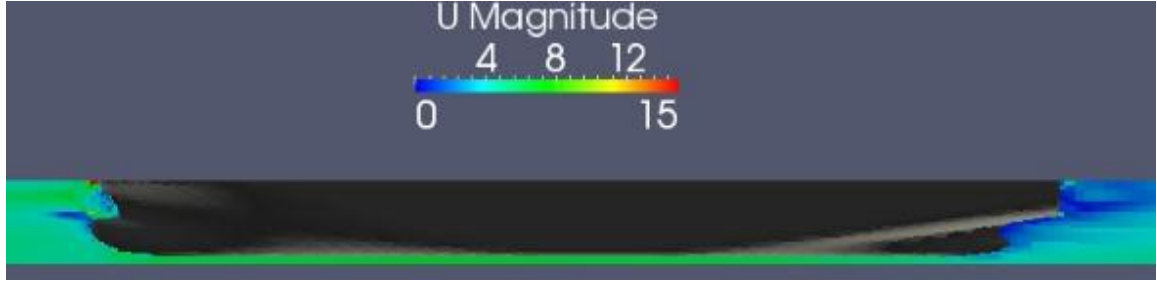


Figure 6.9: Channel fluid velocity (m/s) OpenFOAM, $T=13.0m$, $U=10kn$



Figure 6.10: Channel fluid velocity (m/s) OpenFOAM, $T=14.5m$, $U=10kn$

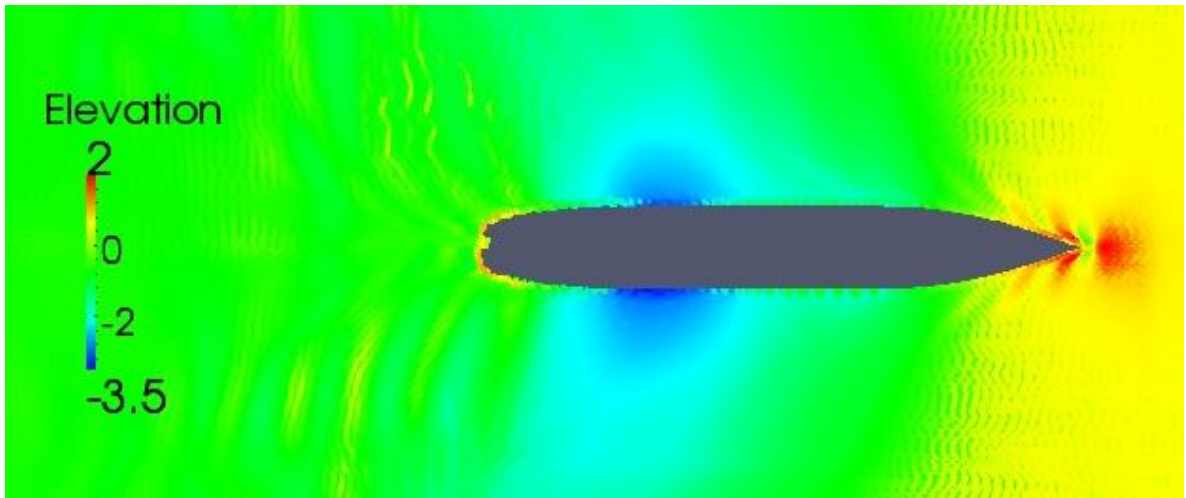


Figure 6.11: Channel elevation and wave pattern, $T=14.5m$, $U=14kn$

The reasons for the discrepancies between OpenFOAM and the experimental data are mainly due to the coarse mesh. In most cases only one cell could fit in the gap between the hull and seabed. This meant that the RANS and other equations were solving values over a

large range. Also the boundaries of that range were different because one was moving at full speed while the other was stationary. The mesh at the bow is rough and this will affect the fluid properties and modeling further down the length of the ship. Another reason for the error is because the stepped channel used in OpenFOAM is actually different to that used in the experiments. It was in fact a ramp like channel as shown in Figure 6.12 and this was difficult to set up in the blockMeshDict and OpenFOAM in general. So the flow around the ship and results obtained would both be different.

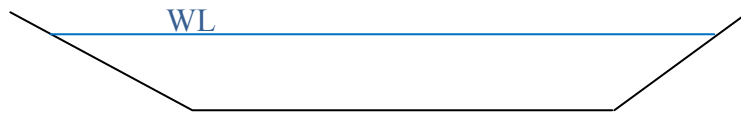


Figure 6.12: Actual channel geometry used in experiments

6.2 Resistance

As mentioned in the previous chapter post-processing the results from OpenFOAM provided the pressure and viscous forces in the x-direction, hence the resistance. This section examines the container ship in deep and shallow water. Again the same draughts and similar speeds are used, with the components of resistance and in some cases the coefficients being calculated. The wave and viscous resistance add up to the total resistance values. Also figures for the free surface elevation and wave pattern are provided for some cases. The accuracy of OpenFOAM was again compared with the other programs and experimental results.

6.2.1 Deep Water

The results from OpenFOAM and the comparison programs for draughts of 14.0m and 14.5m are given in the following tables. All values are in Newtons and the speeds are in knots.

Table 6.3: Deep water resistance OpenFOAM, T=14.0m

Speed (knots)	R_w	R_v	R_T
10	1.01E+06	6.42E+05	1.65E+06
15	2.50E+06	1.10E+06	3.60E+06
20	3.24E+06	1.71E+06	4.96E+06

Table 6.4: Deep water resistance comparison, T=14.0m

Speed (kn)	Maxsurf			Michlet		
	R_w	R_v	R_T	R_w	R_v	R_T
10	2.22E+06	4.55E+05	2.62E+06	1.94E+05	4.63E+05	6.58E+05
15	4.34E+06	1.95E+06	6.05E+06	1.04E+06	9.92E+05	2.03E+06
20	1.77E+06	1.68E+06	3.24E+06	2.77E+06	1.71E+06	4.48E+06

Table 6.5: Deep water resistance OpenFOAM, T=14.5m

Speed (knots)	R_w	R_v	R_T
10	1.29E+06	6.78E+05	1.97E+06
15	2.28E+06	1.13E+06	3.41E+06
20	3.42E+06	1.78E+06	5.20E+06

Table 6.6: Deep water resistance comparison, T=14.5m

Speed (kn)	Maxsurf			Michlet		
	R_w	R_v	R_T	R_w	R_v	R_T
10	7.78E+05	4.67E+05	1.25E+06	2.03E+05	4.76E+05	6.79E+05
15	1.20E+06	1.00E+06	2.20E+06	1.07E+06	1.02E+06	2.09E+06
20	1.32E+06	1.72E+06	3.04E+06	2.94E+06	1.76E+06	4.70E+06

Tables 6.3 to 6.6 show good consistency between OpenFOAM and the other programs for the viscous resistance. With the difference between values being zero for one case

($T=14.0\text{m}$, $U=20\text{kn}$), but more appropriately a minimum of 1.8% difference and maximum of 41%. The wave resistance results are further apart, but they can still be considered to be similar. Some values are more than double making the difference vast, however for such large values of resistance (10^6) the error in measurement will compound and be larger so it can be slightly excused. The results for viscous flow are promising for such a coarse grid. However this is where the close comparison of values between programs starts and stops being a good thing. Both Maxsurf and Michlet use Michell's thin ship theory for calculating the wave resistance. And for the container ship (where C_B equals 0.645) used in this project the large bulb at the bow of the ship affects the accuracy of Michell's integral. This is because a stagnation point forms where the pressure is high and velocity of the fluid is zero. This is best seen in Figures 6.8 and 6.9, even though this is a channel it is the same for deep water. Michell's thin ship theory has a problem with this and instead of waves cancelling out which is what the bulb is used for, instead it increases the wave resistance values. Therefore the wave resistance values calculated by Maxsurf and Michlet, hence by way of comparison also OpenFOAM, are mostly incorrect and not very accurate. However the thin ship theory still applies for this hull shape everywhere else because the beam to length ratio is small enough for the use of the slender body theory. And where slender body is used so can the thin ship theory be used (Tuck and Stokes 2012, 190).

This problem will also affect the free surface wave pattern which utilises the same theory. Figures 6.13 to 6.21 show the free surface for three speeds at a draught of 14.5m. The values for elevation are not at all similar between OpenFOAM and the others especially Michlet. OpenFOAM calculates the elevation to be largest at the bow. Michlet does not determine the near field waves, those closest to the ship. Although these particular waves are in close resemblance between OpenFOAM and Maxsurf. They are closer together at 20knots, however they separate further apart as the speed increases. The far field waves are further from the ship and OpenFOAM also calculates these to be similar to the other programs. It is difficult to distinguish the transverse and diverging waves from the

OpenFOAM results. Transverse waves are the vertical lines in the figures and travel along the length of the hull and then continue on after the stern. The displacement of the wave crest and trough is perpendicular to the ships direction of motion. Diverging waves travel outwards from the bow and stern to form the V shape shown. Only at 25knots were the diverging waves visible from the data gathered by OpenFOAM. At lower speeds the wave resistance is less significant, which is demonstrated in Figures 6.22 and 6.23. There seems to be no wave pattern forming only a small wake will form after the stern as the boundary layer separates. Therefore most of the resistance is viscous which can actually be noted in the shallow water resistance values which run at lower velocities.

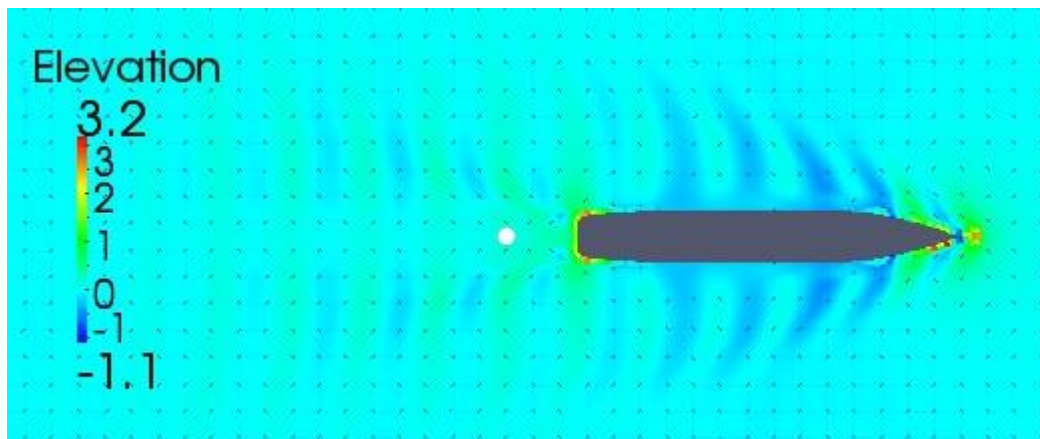


Figure 6.13: Free surface elevation and wave pattern OpenFOAM, $T=14.5m$,
 $U=20kn$

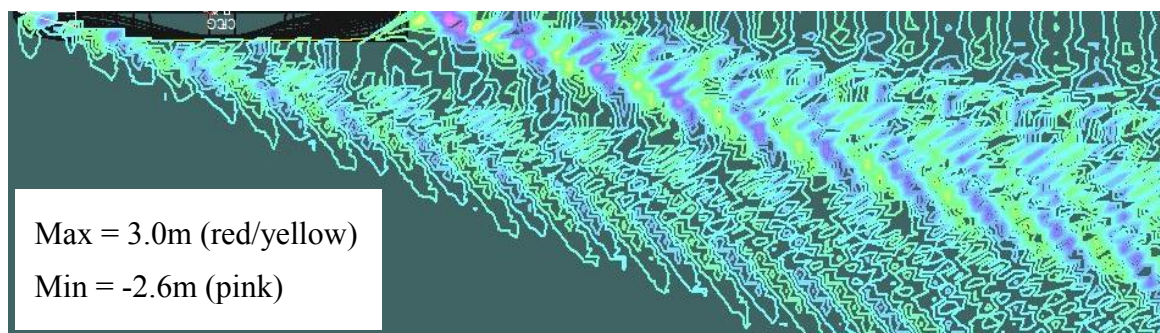


Figure 6.14: Free surface elevation and wave pattern Maxsurf, $T=14.5m$,
 $U=20kn$

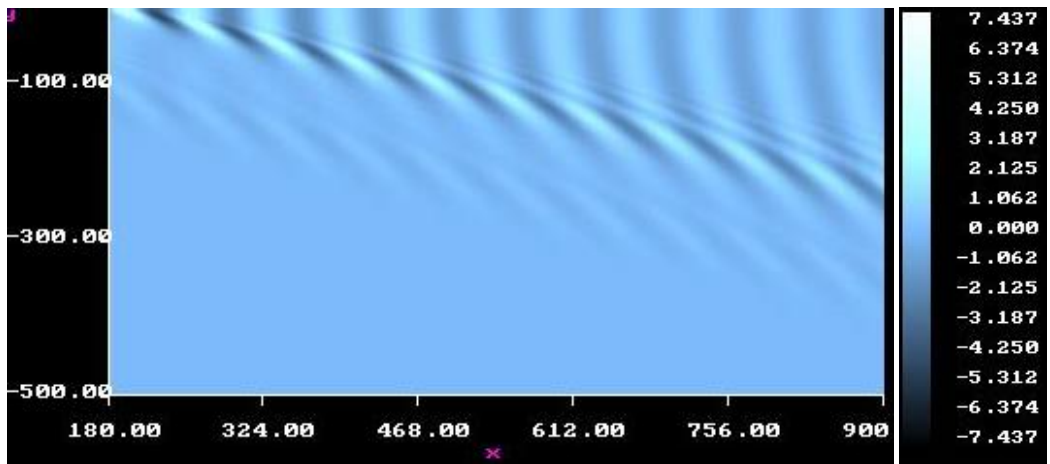


Figure 6.15: Free surface elevation and wave pattern Michlet, $T=14.5m$, $U=20kn$

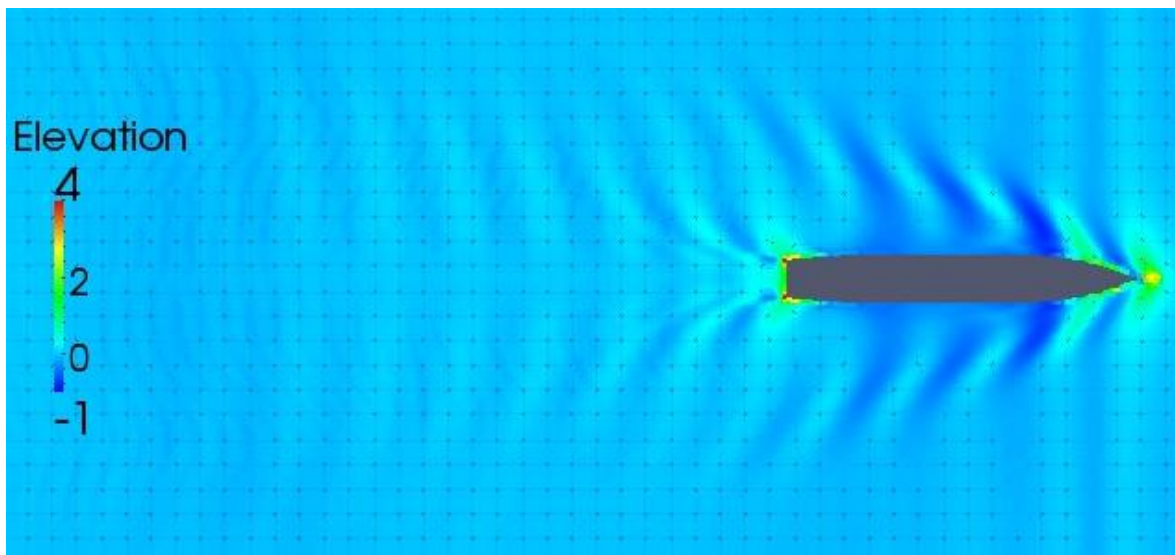


Figure 6.16: Free surface elevation and wave pattern OpenFOAM, $T=14.5m$, $U=22kn$

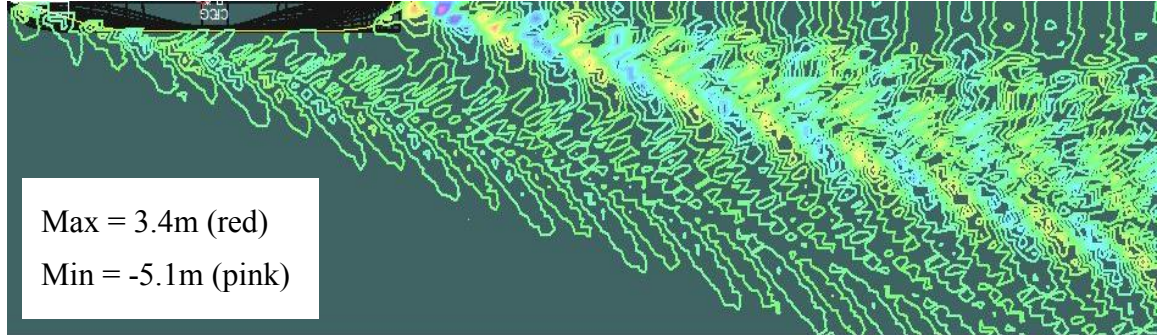


Figure 6.17: Free surface elevation and wave pattern Maxsurf, $T=14.5m$, $U=22kn$

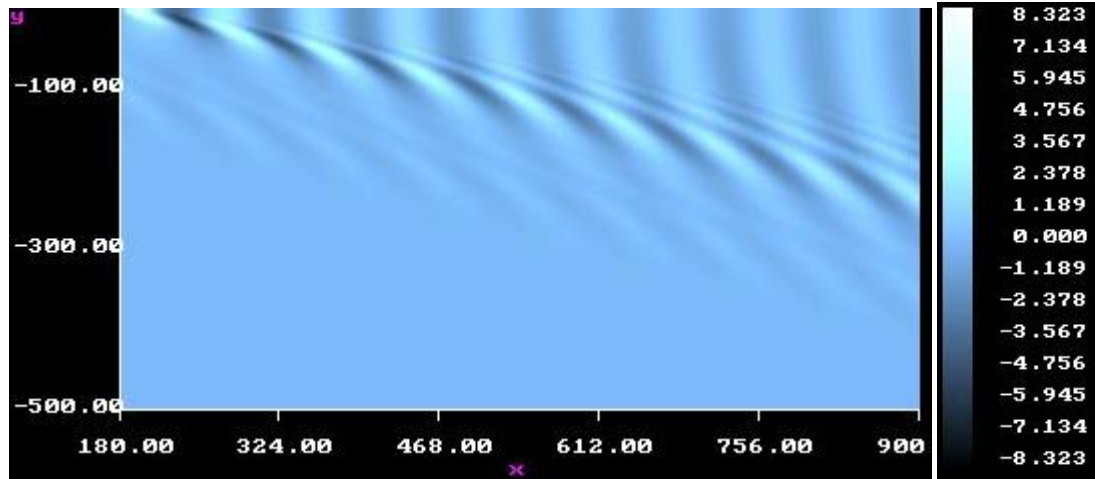


Figure 6.18: Free surface elevation and wave pattern Michlet, $T=14.5m$, $U=22kn$

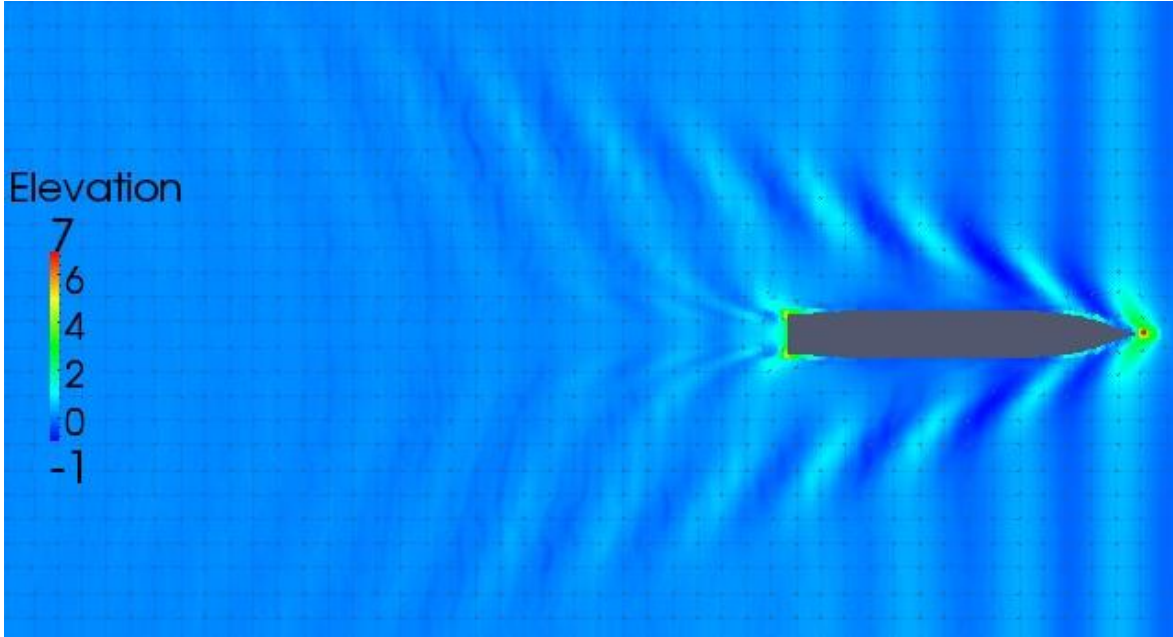


Figure 6.19: Free surface elevation and wave pattern OpenFOAM, $T=14.5m$, $U=25kn$

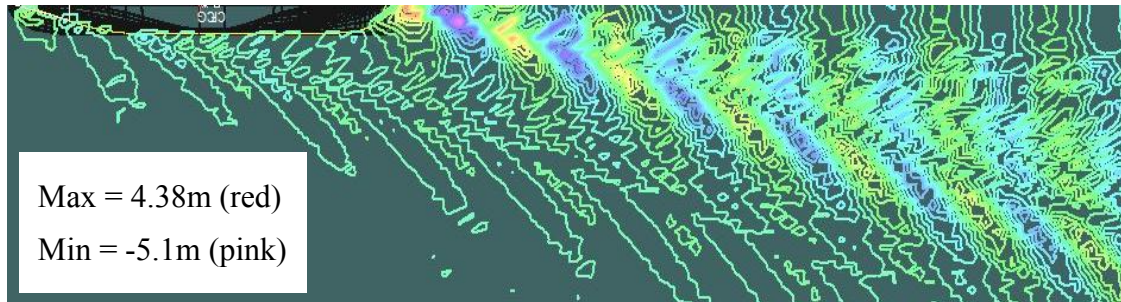


Figure 6.20: Free surface elevation and wave pattern Maxsurf, $T=14.5m$, $U=25kn$

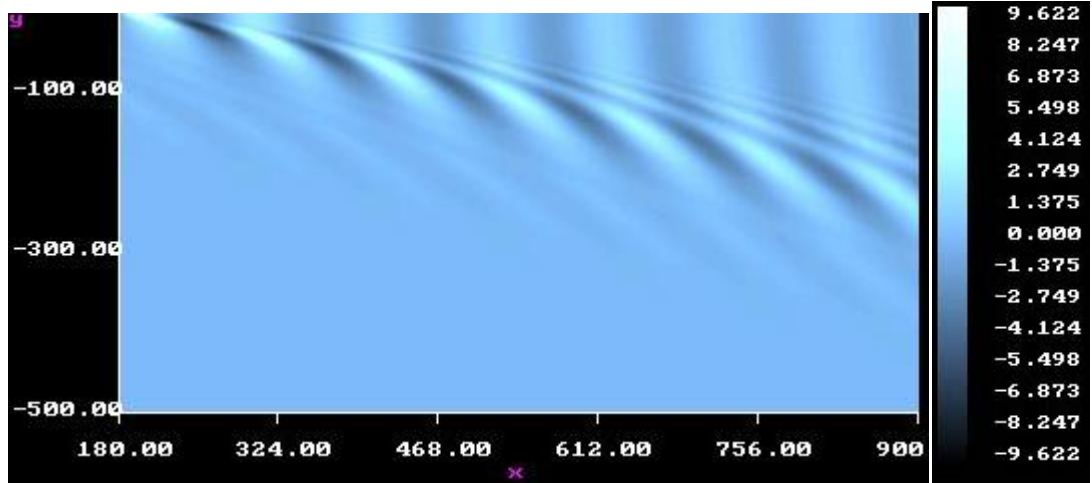


Figure 6.21: Free surface elevation and wave pattern Michlet, $T=14.5m$, $U=25kn$

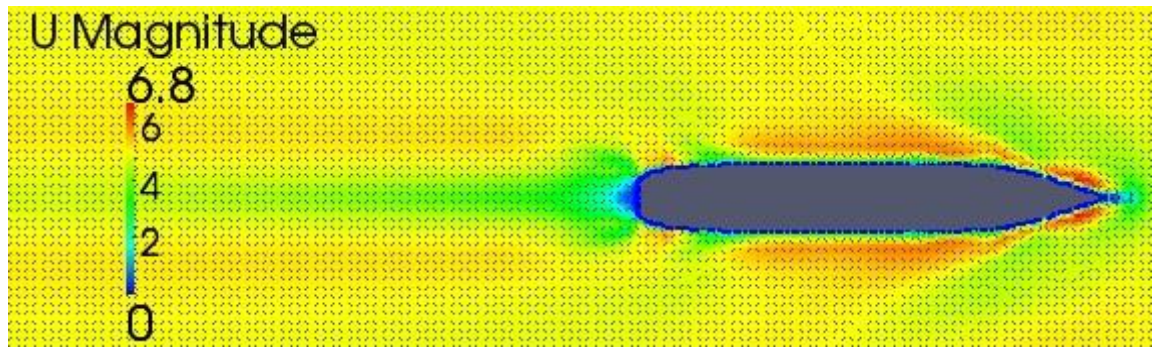


Figure 6.22: Free surface wave pattern and velocity magnitude, $T=14.0m$, $U=10kn$

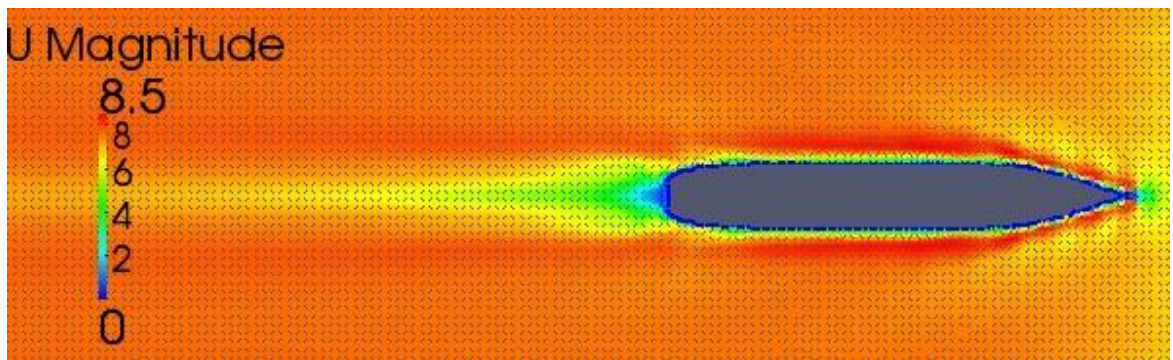


Figure 6.23: Free surface wave pattern and velocity magnitude, $T=14.0m$, $U=15kn$

As mentioned before the wave resistance values obtained are far too large for this particular hull shape. This is further verified by the experimental results from (Moctar, Shigunov and Zorn 2012, 50) as shown in Table 6.7. Here the wave coefficient calculated by OpenFOAM is roughly 15 times larger than the experimental data. Therefore there must be a reason for this large error, and this is again mostly due to the coarse grid. In fact for the number of cells used the mesh could be considered to be very coarse. Even though refinement was done on the free surface, this was not enough. Refinement should have also been done all over the hull surface. The boundary conditions selected for the sides should not have affected the results because they were far enough away from the ship to cause any error.

In (Hanninen and Mikkola n.d.) the effect of the grid size used in the mesh is examined. Although this paper used the Hamburg Test Case which has dimensions roughly half that of the Duisburg Test Case, it is still a container ship with a C_B of 0.645 which is identical to the ship in this report. They determined that the wave coefficient for a medium sized grid was roughly 75% smaller than that of a course grid. The fine grid was then a further 5% smaller than the medium grid. Furthermore they also concluded that the viscous resistance is independent of the size of the mesh, which alludes to these values calculated from OpenFOAM to be fairly accurate. Also (Larsson, Stern and Bertram 2003, 63) found the wave coefficient to be roughly 10-15 times smaller than the viscous coefficient when they used the KRISO containership ($C_B=0.65$).

Table 6.7: Deep water resistance coefficients OpenFOAM, T=14.5m

Speed (kn)	Fr	Re	C_T	C_V	C_W	Exp C_W
20	0.173	3.72E+09	4.62E-03	1.58E-03	3.04E-03	1.93E-04
22	0.190	4.09E+09	4.04E-03	1.43E-03	2.61E-03	1.79E-04
25	0.216	4.65E+09	3.70E-03	1.46E-03	2.24E-03	3.36E-04

Table 6.8: Deep water resistance coefficients comparison, T=14.5m

Speed (kn)	Maxsurf			Michlet		
	C_T	C_V	C_W	C_T	C_V	C_W
20	2.91E-03	1.34E-03	1.17E-03	4.17E-03	1.56E-03	2.61E-03
22	2.97E-03	1.32E-03	1.25E-03	4.39E-03	1.54E-03	2.85E-03
25	3.36E-03	1.30E-03	1.66E-03	5.00E-03	1.52E-03	3.48E-03

6.2.2 Shallow Water

The results in this section are for shallow water with a depth of 16.0m. Almost all other things relating to the set up of the simulation is the same as the deep water cases. Again the wave and viscous resistances are separated and then added together to give the total resistance. Maxsurf cannot be used as a comparison because it doesn't do shallow water models.

As expected the viscous resistance is larger at the lower speeds, however this only occurs for the 14.0m draught and at 6 and 10knots using OpenFOAM. This is because the wave resistance has been over predicted again, and the viscous resistance should be much larger especially at these low Froude numbers. Also the wave resistance values fluctuate between iterations for one case and for speeds of different cases. Hence these values may not be fully converged, however further iterations proved to be mostly unhelpful in solving this problem. So in order to achieve better results a finer mesh must be used. Some patterns that occur between the two draughts include 14.0m having lower wave resistance but higher viscous resistance. This could be possibly true or it could be due to large inconsistencies in the mesh making this an invalid assumption.

The comparison with Michlet shows the same conclusion that was made for deep water in respect to the wave resistance. The viscous values are between 54% and 84% larger in OpenFOAM which is not as close as the deep water results. This is expected because the shallow water conditions will make it harder to be as accurate. Also the dynamic pressure

for the shallow water should be slightly less than the restricted channel, because the sinkage and trim will be smaller. This is demonstrated in Figure 6.24 where the negative pressure is smaller for the same data point in the channel (Figure 6.1).

Table 6.9: Shallow water resistance, T=14.0m

Speed (kn)	OpenFOAM			Michlet		
	R_w	R_v	R_T	R_w	R_v	R_T
6	1.50E+05	3.18E+05	4.68E+05	2.20E+04	1.77E+05	1.99E+05
10	3.97E+05	7.13E+05	1.11E+06	1.93E+05	4.62E+05	6.55E+05
14	2.48E+06	1.60E+06	4.08E+06	7.21E+05	8.70E+05	1.59E+06

Table 6.10: Shallow water resistance, T=14.5m

Speed (kn)	OpenFOAM			Michlet		
	R_w	R_v	R_T	R_w	R_v	R_T
6	3.14E+05	2.48E+05	5.62E+05	2.30E+04	1.83E+05	2.06E+05
10	1.19E+06	6.80E+05	1.87E+06	1.98E+05	4.78E+05	6.76E+05
14	2.64E+06	1.45E+06	4.08E+06	7.46E+05	8.98E+05	1.64E+06

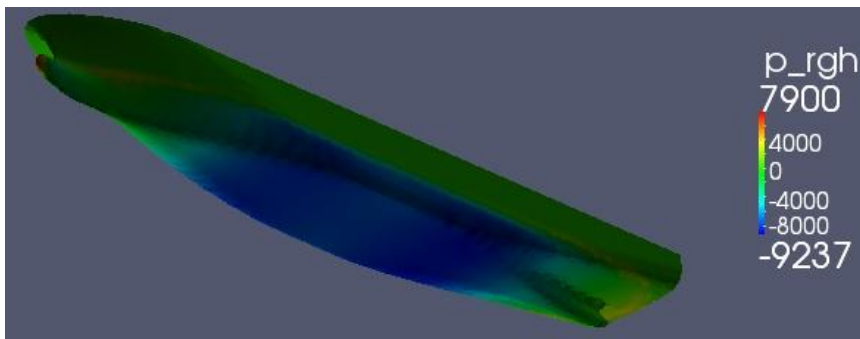


Figure 6.24: Shallow water dynamic pressure, T=14.0m, U=10kn

6.3 Model Scale in Shallow Water

This model scale numerical analysis uses the alternative benchmark experiments done for a 14.0m draught container ship. The experiments use a towing tank that simulates shallow water at 0.4m and a scale model that has dimensions according to the ratio 1:40. Full scale simulations in OpenFOAM would have only been able to calculate values for the trim and wave resistance that could be compared to the scale model experiments. Therefore a geometry and mesh was made up that had the same number of cells as the full scale shallow tests.

The results provide the same resolution as the others carried out in the project. Only the trim has been calculated for the first time in these particular cases. So examining this first shows the values for trim are given in minutes. The OpenFOAM value achieved for the intermediate speed was 11.3 times larger than the experimental. Hence it is not particular good at predicting pitch and moments of the ship. Examining the sinkage shows promising results with OpenFOAM determining a value at the intermediate speed that is 29% higher than the experimental. Again the pattern occurs at higher speeds where OpenFOAM calculates a smaller sinkage. These values mirror the good results obtained from squat predictions in the restricted channel. Finally the resistance also shows the same outcomes as before, where the wave resistance is extremely over estimated. The Froude number for 1.027m/s is only 0.109 and for these very low speeds the resistance should be majority viscous. Therefore comparing the viscous resistance obtained from OpenFOAM at 0.791m/s with the total resistance from the experiments shows there is a difference of 5.7N. Based on the deep water experimental results for a Fr of 0.174 the friction coefficient was 16 times larger than the wave coefficient. And for speeds below this the difference will be even larger. Dividing 23.69 by 16 gives 1.48(N) hence ignoring the wave resistance determined in OpenFOAM and assuming the 5.7N is the wave resistance, the viscous resistance calculated in OpenFOAM is slightly smaller than it should be.

Table 6.11: Model scale in shallow water OpenFOAM, T=0.35m

	OpenFOAM					Experimental		
Speed (m/s)	R_w	R_v	R_T	Trim (1/60)°	Sinkage (mm)	R_T	Trim (1/60)°	Sinkage (mm)
0.4066	10.03	8.627	18.66	0.043	7.99			
0.791	33.60	23.69	57.28	0.113	15.17	29.39	0.01	11.8
1.027	108.8	43.73	152.5	0.325	23.95	68.82	0.95	26.4

7.0 Conclusions and Recommendations

7.1 Conclusions

The objectives set out at the start of this report required the calculation of squat, trim and resistance values for a number of different situations. All of those that were listed have all been modeled and simulated using OpenFOAM. The results provide valuable conclusions on the effectiveness of CFD and OpenFOAM in ship hydrodynamics. It was noticed that almost all values obtained have large errors involved that decrease the accuracy when compared to other methods like experimental data. Therefore the results calculated in this project are not the final outcome of the numerically solving software OpenFOAM. Further analysis is absolutely required and the specifics of this are outlined in the recommendations. This section will provide the observations on suitability of the CFD techniques used and the results achieved in the project.

OpenFOAM does quite a good job at calculating the dynamic pressure on the hull considering the small clearance between the hull and seabed. Particularly for the coarse mesh used and having only one cell making up this clearance, the figures and values obtained on the distribution of dynamic pressure result in the restricted channel squat for intermediate speed and draught being within 24% of experimental data and 29% for the scaled down model in shallow water. OpenFOAM overestimates the pressure on the hull leading to larger squat values. However the software does do well at calculating the fluid velocity around the hull, mimicking the theory of sinkage and trim. The program does have some slight drawbacks in the creating of the geometry and meshing it. The proper ramp channel used in the benchmark experiments was difficult to model in OpenFOAM using the blockMesh utility. The meshing was very good on the simple surfaces of the hull, however the snappyHexMesh utility defaulted to poor breaking up of cells on curved surfaces like the bulb and rudder areas. In order to make these cells smoother a lot of refinement was required. However the finer the mesh became the more time consuming the simulation was

to run. So there has to be a good balance between accuracy and time, and unfortunately this project leaned towards small simulation times.

Drawing on the conclusions from calculating the force in the z-direction for squat, it can easily be determined from the resistance results that the forces in the x-direction are definitely not as accurate. This is most evident in the extreme error involved with the wave resistance. The viscous resistance however is quite accurate and in close proximity to the other programs and experimental data. It is the wave resistance though that is of most concern. OpenFOAM overestimates the values by large amounts; this is obvious because the viscous resistance should be much larger than the wave resistance for container ships, however in most cases it is the other way round. At all speeds, draughts and depth of water the results of wave resistance are incorrect. Shallow water cases have trouble with finding a final value, with data fluctuating between iterations even after a large amount of time steps. The setting up of the multiphase model with the parameter alpha was difficult because the boundary conditions had to be interchanged between 1 and 2 inlets to suit the case. It seems though that the mesh is the main culprit for the large error in resistance. The cells near the bow, stern and free surface of the hull need to be extra refined in order to obtain an appropriate result. Hence large computation times are required for determining accurate wave resistance values in OpenFOAM.

Overall the above resolutions show there are promising prospects for OpenFOAM and CFD in calculating ship hydrodynamics. CFD seems to be better for container ships than other mathematical programs like Maxsurf and Michlet, because of the shape of the hull including the bulb. With more advanced computer systems and better meshing of full scale large structures the CFD approach will eventually become the better option over model testing in towing tanks especially for large container ships. However there is still a long way to go before numerical techniques are accurate and the results are considered feasible and trustworthy.

7.2 Recommendations

The following recommendations are based on the conclusions from the project and what further advancements need to be made. They are there as a guide to the next person who wishes to explore the abilities of OpenFOAM and CFD techniques. The work done on the following points will hopefully provide better results and outcomes that can be accurately matched with experimental data.

1. More refinement of the mesh around the edges of the hull, focusing on the bulb, stern, sharp edges and free surface interface between air and water. The mesh also needs to be finer underneath the hull for squat predictions and generally overall especially in shallow water.
2. A further comparison between full scale and model scale simulations. It would be interesting to see which is the more accurate and is better modeled in OpenFOAM.
3. Include appendages such as rudders and propellers so as to provide a more complete picture on the overall forces on the ship.
4. Determine other methods for generating the geometry of the channel so the ramped sides can be modeled without worrying about the accuracy.
5. Explore some different boundary conditions in the set up of the numerical model. The most appropriate would be to determine what difference in data there is between having one inlet with a predetermined separation of the two fluids and two inlets where one is water and the other is air.
6. Create OpenFOAM utilities that calculate the sinkage, trim, resistance and hydrostatics like waterplane area, displacement, MTC and second moment of areas. It would also be useful if the ship was modeled in waters that are not calm. This will provide results on wave motions such as heave, pitch, roll and a number of other stability parameters like metacentric height and heel angle.

8.0 References

- Aktar, Salina, Goutam Kumar Saha, and Abdul Alim. "Drag Analysis of Different Ship Models Using Computational Fluid Dynamic Tools." *The International Conferance of Marine Technology*, 2010.
- Anderson Jr, J D. *Computational Fluid Dynamics An Introduction*. Springer, 2009.
- Andersson, Bengt, Ronnie Andersson, Love Håkansson, Mikael Mortensen, Rahman Sudiyo, and Berend Van Wachem. *Computational Fluid Dynamics for Engineers*. Cambridge: Cambridge University Press, 2011.
- Barrass, C B, and D R Derrett. *Ship Stability for Masters and Mates*. Elsevier, 2012.
- Barrass, C B, and P J Helmore. "Determination of Coefficient K for Prediction of Ship Squat." 2004.
- Biran, Adrian. *Ship Hydrostatics and Stability*. Butterworth-Heinemann, 2003.
- Briggs, Michael J. *Ship Squat Predictions for Ship/Tow Simulator*. US Army Corps of Engineers, 2006.
- Callister Jr, William D. *Materials Science and Engineering an Introduction*. New York: John Wiley & Sons, 2007.
- Colley, Eamonn. *Analysis of Flow Around a Ship Propeller using OpenFOAM*. Thesis, Curtin University, 2012.
- Dick, E. *Computational Fluid Dynamics An Introduction*. Springer, 2009.
- Dunker, Sven. "Analysis of Waterway Factors on the Underkeel Clearance of Sea-going Vessels." *Squat Workshop, Elsfleth/Oldenburger (Germany)* , 2004: 150-172.
- Dunker, Sven, Andreas Gollenstede, Alexander Härting, and Jörg Reinking. "Analysis and Comparison of SHIPS Derived Squat." 2002.
- Eloot, Katrien, Jeroen Verwilligen, and Marc Vantorre. "An Overview Of Squat Measurements For Container Ships In Restricted Water." *SOCW*, 2008: 106-116.
- Gourlay, T P. "A brief history of mathematical ship-squat prediction, focussing on the contributions of E.O. Tuck." *Journal of Engineering Mathematics*, 2011 (70): 5-16.
- Gourlay, T P. "A Simple Method for Predicting the Maximum Squat of a High Speed Displacement Ship." *Marine Technology*, 2006 (43): 146-151.
- Gourlay, Tim. "Slender-Body Methods for Predicting Ship Squat." *Ocean Engineering*, 2008 (35): 191-200.
- Gourlay, Tim, and Kim Klaka. "Full Scale Measurments of Containership Sinkage, Trim and Roll." *Australian Naval Architect*, 2007 (11): 30-36.
- Grigson, C W. "A planar friction algorithm and its use in analysing hull resistance." *Trans. RINA*, 2000: 76-115.

Hanninen, Satu, and Tommi Mikkola. *Computation of Ship-Hull Flows at Model and Full-Scale Reynolds Numbers*. Ship Laboratory, Helsinki University of Technology.

Harting, Alexander, and Jorg Reinking. "SHIPS: A New Method for Efficient Full Scale Ship Squat Determination." 2000.

Hochkirch, Karsten, and Benoit Mallol. *On the importance of full-scale CFD simulations for ships*. Numeca, 2012.

Hughes, G. "Correlation of Model Resistance and Application to Ships." *R.I.N.A.*, 1963.

ITTC. *Recommended Procedures: Resistance Uncertainty Analysis, Example for Resistance Test*. Venice: 23rd International Towing Tank Conference, 2002.

Katsui, T, H Asai, Y Himeno, and Y Tahara. "The Proposal of a New Friction Line." *Fifth Osaka Colloquium on Advanced CFD Applications to Ship Flow and Hull Form Design*, 2005.

Larsson, Lars, Frederick Stern, and Volker Bertram. "Benchmarking of Computational Fluid Dynamics for Ship Flows: The Gothenburg 2000 Workshop." *Journal of Ship Research*, 2003 47(1): 63-81.

Lazauskas, L, and E O Tuck. *Unconstrained Ships of Minimum Total Drag*. University of Adelaide, 1996.

Lazauskas, Leo V. *Resistance, Wave-Making and Wave-Decay of Thin Ships with Emphasis on the Effects of Viscosity*. Thesis, University of Adelaide, 2009.

Malalasekera, W, and H K Versteeg. *An Introduction to Computational Fluid Dynamics*. Pearson, 2007.

Michaud, S, B Morse, R Santerre, A Taschereau, and J Siles. "Precise Determination of Vessel Squat and Under-keel Clearance." *4th Transportation Specialty Conference*, 2002.

Michell, J H. "The Wave-Resistance of a Ship." *Philosophical Magazine*, 1898 (45): 106-123.

Moctar, Ould el, Vladimir Shigunov, and Tobias Zorn. "Duisburg Test Case: Post-Panamax Container Ship for Benchmarking." *Ship Technology Research*, 2012 (59): 50-65.

Morse, Brian, Stephanie Michaud, Andre Taschereau, and Rock Santerre. "Ship squat in shallow and confined channels - the Canadian experience." *Squat Workshop, Elsfleth/Oldenburger (Germany)*, 2004.

Munson, B R, D F Young, and T H Okiishi. *Fundamentals of Fluid Mechanics*. New York: John Wiley, 1998.

OpenFOAM Foundation. "OpenFOAM User Guide." 2011. <http://www.openfoam.org/docs/user/> (accessed May 5, 2013).

PIANC-IAPH. "Approach Channels, A Guide for Design." *PIANC-Bulletin*, 1997.

- "Pre Squat." *University of Duisburg-Essen*. 2013. http://www.uni-due.de/IST/ismt_presquat.shtml (accessed April 1, 2013).
- Prohaska, C W, and L Landweber. *Resistance Session: Report of Resistance Committee*. ITTC.
- Raven, H C, A Van Der Ploeg, and A R Starke. "Towards a CFD based prediction of ship performance - Progress in predicting full-scale resistance and scale effects." *MARIN*.
- Read, Douglas. *A Drag Estimate for Concept-Stage Ship Design Optimisation*. Thesis, Maine: B. S. Webb Institute, 1997.
- The Nautical Site*. <http://thenauticalsite.com/NauticalNotes/Stability/MyStability-Lesson09-Trim.htm> (accessed May 5, 2013).
- Tuck, E O. "Hydrodynamic problems of ships in restricted waters." *Ann Rev Fluid Mechanics*, 1978 (10): 33–46.
- Tuck, E O. "Sinkage and trim in shallow water of finite width." *Schiffstechnik*, 1967 (14): 92–94.
- Tuck, E O. *Wave Resistance of Thin Ships and Catamarans*. University of Adelaide, 1997.
- Tuck, E O, and Y M Stokes. "On Thin or Slender Bodies." *ANZIAM Journal*, 2012 53(3): 190-212.
- Tuck, E O, R F Beck, and J N Newman. "Hydrodynamic forces on ships in dredged channels." *J Ship Res*, 1975 (19): 166–171.
- Tupper, E C. *Introduction to Naval Architecture*. Amsterdam: Butterworth Heinemann, 2004.
- Walshaw, A C, and D A Jobson. *Mechanics of Fluids*. Longmans, 1965.
- Zhang, Zhi-rong. "Verification and Validation for RANS simulation of KCS container ship without/with propeller." *Journal of Hydrodynamics*, 2010 22(5): 932-939.
- Zhang, Zhi-rong, Hui Liu, Song-ping Zhu, and Feng Zhao. "Application of CFD in ship engineering design practice and ship hydrodynamics." *Journal of Hydrodynamics*, 2006 18(3): 315-322.

Appendix A: Equations

Momentum equations in y direction,

$$\rho g_y + \frac{\partial(\tau_{xy})}{\partial x} + \frac{\partial(\sigma_{yy})}{\partial y} + \frac{\partial(\tau_{zy})}{\partial z} = \rho \left(\frac{\partial v}{\partial t} + u \frac{\partial v}{\partial x} + v \frac{\partial v}{\partial y} + w \frac{\partial v}{\partial z} \right) \quad (\text{A1})$$

And in the z direction,

$$\rho g_z + \frac{\partial(\tau_{xz})}{\partial x} + \frac{\partial(\tau_{yz})}{\partial y} + \frac{\partial(\sigma_{zz})}{\partial z} = \rho \left(\frac{\partial w}{\partial t} + u \frac{\partial w}{\partial x} + v \frac{\partial w}{\partial y} + w \frac{\partial w}{\partial z} \right) \quad (\text{A2})$$

Normal stresses in the x direction,

$$\sigma_{xx} = -p + 2\mu \frac{\partial u}{\partial x} \quad (\text{A3})$$

Shear stresses for the x direction,

$$\tau_{yx} = \mu \left(\frac{\partial u}{\partial y} + \frac{\partial v}{\partial x} \right) \quad (\text{A4})$$

$$\tau_{zx} = \mu \left(\frac{\partial w}{\partial x} + \frac{\partial u}{\partial z} \right) \quad (\text{A5})$$

Navier-Stokes equation in the y direction,

$$\rho g_y - \frac{\partial p}{\partial y} + \mu \left(\frac{\partial^2 v}{\partial x^2} + \frac{\partial^2 v}{\partial y^2} + \frac{\partial^2 v}{\partial z^2} \right) = \rho \left(\frac{\partial v}{\partial t} + u \frac{\partial v}{\partial x} + v \frac{\partial v}{\partial y} + w \frac{\partial v}{\partial z} \right) \quad (\text{A6})$$

And in the z direction,

$$\rho g_z - \frac{\partial p}{\partial z} + \mu \left(\frac{\partial^2 w}{\partial x^2} + \frac{\partial^2 w}{\partial y^2} + \frac{\partial^2 w}{\partial z^2} \right) = \rho \left(\frac{\partial w}{\partial t} + u \frac{\partial w}{\partial x} + v \frac{\partial w}{\partial y} + w \frac{\partial w}{\partial z} \right) \quad (\text{A7})$$

RANS equation in the y-direction,

$$\begin{aligned} -\frac{\partial P}{\partial y} + \mu \left(\frac{\partial^2 V}{\partial x^2} + \frac{\partial^2 V}{\partial y^2} + \frac{\partial^2 V}{\partial z^2} \right) - \rho \left(u' \frac{\partial v'}{\partial x} + v' \frac{\partial v'}{\partial y} + w' \frac{\partial v'}{\partial z} \right) \\ = \rho \left(\frac{\partial V}{\partial t} + U \frac{\partial V}{\partial x} + V \frac{\partial V}{\partial y} + W \frac{\partial V}{\partial z} \right) \end{aligned} \quad (\text{A8})$$

And in the z direction,

$$\begin{aligned} -\frac{\partial P}{\partial z} + \mu \left(\frac{\partial^2 W}{\partial x^2} + \frac{\partial^2 W}{\partial y^2} + \frac{\partial^2 W}{\partial z^2} \right) - \rho \left(u' \frac{\partial w'}{\partial x} + v' \frac{\partial w'}{\partial y} + w' \frac{\partial w'}{\partial z} \right) \\ = \rho \left(\frac{\partial W}{\partial t} + U \frac{\partial W}{\partial x} + V \frac{\partial W}{\partial y} + W \frac{\partial W}{\partial z} \right) \end{aligned} \quad (\text{A9})$$

Appendix B: OpenFOAM files

blockMeshDict for OpenFOAM

```
/*-----*- C++ -*-----
--*\
|\\Field      | OpenFOAM: The Open Source CFD Toolbox |
|\\Operation  | Version: 2.2.0 |
|\\And        | Web: www.OpenFOAM.org |
|\\Manipulation | |
\*-----*
--*/
FoamFile
{
    version      2.0;
    format       ascii;
    class        dictionary;
    object       blockMeshDict;
}
// * * * * *
//

convertToMeters 1;

vertices
(
    (-932.0 -128.0 -16.0)
    ( 560.0 -128.0 -16.0)
    ( 560.0 166.0 -16.0)
    (-932.0 166.0 -16.0)
    (-932.0 -128.0 -8.0)
    ( 560.0 -128.0 -8.0)
    ( 560.0 166.0 -8.0)
    (-932.0 166.0 -8.0)
    (-932.0 -288.0 -8.0)
    ( 560.0 -288.0 -8.0)
    ( 560.0 262.0 -8.0)
    (-932.0 262.0 -8.0)
    (-932.0 -128.0 15.499)
    ( 560.0 -128.0 15.499)
    ( 560.0 166.0 15.499)
    (-932.0 166.0 15.499)
    (-932.0 -288.0 15.499)
    ( 560.0 -288.0 15.499)
    ( 560.0 262.0 15.499)
    (-932.0 262.0 15.499)
);
```

```

blocks
(
  hex (0 1 2 3 4 5 6 7) (373 74 2) simpleGrading (1 1 1)
  hex (8 9 5 4 16 17 13 12) (373 40 6) simpleGrading (1 1 1)
  hex (4 5 6 7 12 13 14 15) (373 74 6) simpleGrading (1 1 1)
  hex (7 6 10 11 15 14 18 19) (373 24 6) simpleGrading (1 1 1)
);

edges
(
);

boundary
(
  inlet
  {
    type patch;
    faces
    (
      (1 2 6 5)
      (9 5 13 17)
      (5 6 14 13)
      (6 10 18 14)
    )
  };
}

  outlet
  {
    type patch;
    faces
    (
      (0 3 7 4)
      (8 4 12 16)
      (4 7 15 12)
      (7 11 19 15)
    )
  };
}

  atmosphere
  {
    type patch;
    faces
    (
      (16 17 13 12)
      (12 13 14 15)
      (15 14 18 19)
    )
  };
}

```

```

sides
{
    type patch;
    faces
    (
        (8 9 17 16)
        (8 9 5 4)
        (0 1 5 4)
        (0 1 2 3)
        (3 2 6 7)
        (7 6 10 11)
        (11 10 18 19)
    );
}
);

```

```

//
*****
***

```

fvSchemes for OpenFOAM

```

FoamFile
{
    version      2.0;
    format       ascii;
    class        dictionary;
    location     "system";
    object       fvSchemes;
}
// * * * * *
//

ddtSchemes
{
    default      localEuler rDeltaT;
}

gradSchemes
{
    default      Gauss linear;
}

divSchemes

```

```

{
    div(rho*phi,U) Gauss linearUpwind grad(U);
    div(phi,alpha) Gauss vanLeer;
    div(phirb,alpha) Gauss interfaceCompression;
    div(phi,k) Gauss upwind;
    div(phi,omega) Gauss upwind;
    div((muEff*dev(T(grad(U)))) Gauss linear;
}

laplacianSchemes
{
    default Gauss linear corrected;
}

interpolationSchemes
{
    default linear;
}

snGradSchemes
{
    default corrected;
}

fluxRequired
{
    default no;
    p_rgh;
    pcorr;
    alpha1;
}

//*****
**//

```

fvSolution for OpenFOAM

```

FoamFile
{
    version 2.0;
    format ascii;
    class dictionary;
    location "system";
    object fvSolution;
}

```

```

// * * * * *
//

solvers
{
    pcorr
    {
        solver          PCG;

        preconditioner
        {
            preconditioner  GAMG;

            smoother        DICGaussSeidel;
            agglomerator     faceAreaPair;
            mergeLevels      1;
            nCellsInCoarsestLevel 10;
            cacheAgglomeration true;

            tolerance        1e-5;
            relTol           0;
        };

        tolerance        1e-5;
        relTol           0;
    };

    p_rgh
    {
        solver          GAMG;

        smoother        GaussSeidel;
        agglomerator     faceAreaPair;
        mergeLevels      1;
        nCellsInCoarsestLevel 10;
        cacheAgglomeration true;

        tolerance        1e-6;
        relTol           0.01;
    };

    p_rghFinal
    {
        $p_rgh;
        tolerance        1e-6;
        relTol           0;
    }

    "(U|k|omega).*"

```

```

    {
        solver          smoothSolver;

        smoother        GaussSeidel;
        nSweeps          1;

        tolerance        1e-7;
        relTol           0.1;
    };
}

```

PIMPLE

```

{
    momentumPredictor yes;

    nCorrectors          1;
    nNonOrthogonalCorrectors 0;

    nAlphaCorr           1;
    nAlphaSubCycles      1;
    cAlpha                1;

    maxCo                 0.9;
    maxAlphaCo            0.2;
    nAlphaSweepIter      1;

    rDeltaTSmoothingCoeff 0.1;
    rDeltaTDampingCoeff  1;
    maxDeltaT             1;
}

```

relaxationFactors

```

{
    fields
    {
    }
    equations
    {
    }
}

```

```

//*****
*//

```

Appendix C: Tables of Hydrostatics

Table C.1: Table of offsets, T=14.0m

St/WL	1	2	3	4	5	6	7	8	9	10	11	12	13	14	15	16	17	18	19	20	21
1	0	0	0	0	0	0	0	0	0	0	0	0	0	0	0	0	0	0	0	0	0
2	0	0	0	0	0	0	0	0	0	0	0	0	0.34	0.79	1.10	1.26	1.29	1.13	0.68	0	0
3	0	0.55	1.16	1.71	2.20	2.62	2.98	3.28	3.53	3.72	3.86	3.94	3.98	3.91	3.73	3.46	3.12	2.72	2.38	2.19	2.14
4	0	1.46	2.25	2.84	3.31	3.72	4.07	4.38	4.64	4.87	5.06	5.24	5.43	5.62	5.83	6.06	6.33	6.63	6.96	7.32	7.71
5	0	2.60	3.75	4.59	5.28	5.88	6.41	6.92	7.43	7.92	8.41	8.88	9.35	9.83	10.3	10.8	11.3	11.8	12.4	12.9	13.5
6	0	4.64	6.27	7.51	8.55	9.45	10.3	11.0	11.7	12.4	13.1	13.7	14.3	14.9	15.5	16.1	16.6	17.1	17.6	18.1	18.6
7	0	8.04	10.1	11.6	12.8	13.9	14.8	15.7	16.5	17.1	17.8	18.4	19.0	19.5	20.0	20.5	20.9	21.3	21.7	22.1	22.5
8	0	12.5	14.6	16.1	17.3	18.3	19.2	19.9	20.6	21.1	21.7	22.2	22.6	23.0	23.3	23.6	23.9	24.2	24.4	24.6	24.8
9	0	17.0	18.8	20.1	21.1	21.9	22.5	23.1	23.5	23.9	24.2	24.5	24.7	24.9	25.1	25.2	25.3	25.4	25.4	25.5	25.5
10	0	20.6	22.0	22.9	23.6	24.2	24.5	24.9	25.1	25.3	25.4	25.5	25.5	25.5	25.5	25.5	25.5	25.5	25.5	25.5	25.5
11	0	22.7	23.7	24.4	24.8	25.1	25.3	25.4	25.5	25.5	25.5	25.5	25.5	25.5	25.5	25.5	25.5	25.5	25.5	25.5	25.5
12	0	23.3	24.2	24.7	25.1	25.4	25.5	25.5	25.5	25.5	25.5	25.5	25.5	25.5	25.5	25.5	25.5	25.5	25.5	25.5	25.5
13	0	23.3	24.2	24.7	25.1	25.4	25.5	25.5	25.5	25.5	25.5	25.5	25.5	25.5	25.5	25.5	25.5	25.5	25.5	25.5	25.5
14	18.8	22.7	23.7	24.4	24.8	25.2	25.4	25.5	25.5	25.5	25.5	25.5	25.5	25.5	25.5	25.5	25.5	25.5	25.5	25.5	25.5
15	13.3	19.7	21.5	22.7	23.5	24.2	24.7	25.1	25.3	25.4	25.5	25.5	25.5	25.5	25.5	25.5	25.5	25.5	25.5	25.5	25.5
16	0	14.2	16.7	18.7	20.3	21.6	22.6	23.5	24.2	24.7	25.0	25.3	25.4	25.5	25.5	25.5	25.5	25.5	25.5	25.5	25.5
17	3.61	8.85	10.8	12.4	14.0	15.7	17.5	19.3	21.0	22.4	23.3	24.0	24.5	24.9	25.2	25.3	25.4	25.5	25.5	25.5	25.5
18	1.50	5.55	6.86	7.80	8.62	9.44	10.3	11.4	12.9	15.1	17.6	20.0	21.7	22.9	23.7	24.3	24.7	25.0	25.2	25.4	25.4
19	0	3.44	4.27	4.75	5.08	5.37	5.64	5.96	6.34	6.82	7.54	9.13	12.2	15.7	18.6	20.8	22.2	23.2	23.9	24.4	24.8
20	0	2.01	2.58	2.85	2.95	2.93	2.81	2.64	2.48	2.35	2.26	2.26	2.44	2.89	3.96	8.14	12.8	16.6	19.6	21.4	22.7
21	0	0	0	0	0	0	0.28	0.84	0.60	0	0	0	0	0	0	0	0	0	0.11	7.23	14.7

Table C.2: Simpson's rule, T=14.0m

Station	Half Breadth	x	x ²	SM	(B/2).SM	x(B/2).SM	x ² (B/2).SM
1	0.075	180.394	130168.7	1	0.075	27.059175	9762.65269
2	2.396	162.354	117476.9	4	9.584	3284.9064	1125898.39
3	7.833	144.315	105436.6	2	15.666	5086.9069	1651769.53
4	13.434	126.275	94046.49	4	53.736	16479.219	5053682.13
5	18.434	108.236	83307.85	2	36.868	10641.248	3071393.97
6	22.22	90.197	73220.03	4	88.88	24050.217	6507796.31
7	24.599	72.157	63782.51	2	49.198	12425.053	3137972.06
8	25.467	54.118	54996.35	4	101.868	23889.37	5602367.89
9	25.5	36.078	46860.56	2	51	11040.123	2389888.55
10	25.5	18.039	39376.05	4	102	20240.268	4016357.34
11	25.5	0	32542.36	2	51	9200.145	1659660.16
12	25.5	-18.04	26359.15	4	102	16560.21	2688632.89
13	25.5	-36.079	20827.11	2	51	7360.116	1062182.5
14	25.5	-54.119	15945.63	4	102	12880.152	1626454.07
15	25.5	-72.158	11715.25	2	51	5520.087	597477.657
16	25.5	-90.198	8135.499	4	102	9200.094	829820.879
17	25.496	-108.237	5206.777	2	50.992	3679.4807	265503.971
18	25.496	-126.276	2928.866	4	101.984	5519.2721	298697.487
19	24.03	-144.316	1301.694	2	48.06	1733.9567	62559.4252
20	24.03	-162.355	325.4416	4	96.12	1734.0048	31281.4466
21	0	-180.395	0	1	0	0	0
				Σ	1265.031	200551.89	41689159.3

Table C.3: Simpson's rule, T=0.35m

Station	Half Breadth	x	x ²	SM	(B/2).SM	x(B/2).SM	x ² (B/2).SM
1	0.001875	4.50985	81.35553	1	0.001875	0.01691199	0.15254162
2	0.0599	4.05885	73.42313	4	0.2396	2.05306771	17.5921829
3	0.195825	3.607875	65.89795	2	0.39165	3.17931875	25.8089306
4	0.33585	3.156875	58.77913	4	1.3434	10.2995187	78.9638862
5	0.46085	2.7059	52.06748	2	0.9217	6.65078443	47.9905972
6	0.5555	2.254925	45.76259	4	2.222	15.0313967	101.684468
7	0.614975	1.803925	39.86413	2	1.22995	7.76566446	49.0308911
8	0.636675	1.35295	34.37278	4	2.5467	14.9308692	87.5371476
9	0.6375	0.90195	29.2879	2	1.275	6.90008325	37.3420775
10	0.6375	0.450975	24.61008	4	2.55	12.6501803	62.7557099
11	0.6375	0	20.33902	2	1.275	5.750097	25.9322475
12	0.6375	-0.451	16.47451	4	2.55	10.350144	42.0099925
13	0.6375	-0.90198	13.01698	2	1.275	4.60007888	16.5966476
14	0.6375	-1.35298	9.966049	4	2.55	8.05010775	25.4134254
15	0.6375	-1.80395	7.322057	2	1.275	3.45006075	9.33562289
16	0.6375	-2.25495	5.084709	4	2.55	5.7500715	12.9660087
17	0.6374	-2.70593	3.254254	2	1.2748	2.29968183	4.14852254
18	0.6374	-3.1569	1.830555	4	2.5496	3.44955781	4.66718272
19	0.60075	-3.6079	0.813568	2	1.2015	1.08372897	0.97750186
20	0.60075	-4.05888	0.203406	4	2.403	1.08376502	0.48878344
21	0	-4.50988	2.5E-11	1	0	0	0
				Σ	31.62577	125.345089	651.394368

Appendix D: Michlet Input File

```
# =====  
# Project, 14.0m  
#  
# ===== INPUT FILE TYPE AND SUBTYPE =====  
# Input File Type (0=Standard)  
0  
# Input File Subtype (0=Standard)  
0  
# ===== OUTPUT FILE TYPE AND SUBTYPE =====  
# Output File Type (0=Standard)  
0  
# Output File Subtype (0=Standard)  
0  
# ===== COURSE AND VESSEL TYPE =====  
# Course Particulars (0=None)  
0  
# Number of Hulls (1, 2,..., or 5)  
1  
# ===== PHYSICAL QUANTITIES =====  
# Gravitational Acceleration (m/sec/sec) (min 9.6, max 9.9)  
9.80665  
# ===== WATER PROPERTIES =====  
# Water Density (kg/cubic metre) (min 995.0, max 1030.0)  
1000.0  
# Water Kin. Viscosity (sq. m/sec * 10^-6) (min 0.5, max 2.0)  
1.0  
# Base Eddy Kin. Viscosity (non-dimensional, min 1.0)  
10.0  
# Water Depth (metres) (max=10000.0)  
500.0  
# ===== AIR PROPERTIES =====  
# Air Density (kg/cubic metre) (min 0.9, max 2.0)  
1.0  
# Air Kin. Viscosity (sq. m/sec * 10^-6) (min 10.0, max 20.0)  
14.8  
# Wind Speed (m/sec)  
0.0  
# Wind Direction (degrees)  
0.0  
# ===== CALCULATION PARAMETERS =====  
# Minimum Speed (m/sec) (min 0.01, max 51.9)  
0.01  
# Maximum Speed (m/sec) (max 52.0)  
13.0
```

```

# Number of Speeds (min 2, max 101)
100
# Leeway Parameters (0=None)
0
# Wave Drag Ntheta
512
# Skin Friction Method (0=None, 1=ITTC1957, 2=Grigson)
1
# Viscous Form Factor Method (0=None, 3=Dual)
3
# Viscous Drag Form Factor
1.145
# Wave Drag Form Factor
1.0
# Pressure Signature Method (0=None,1=Slender body)
1
# ===== SHIP CALCULATION PARAMETERS =====
# Number of Offset Stations (rows) (odd integer: min 5, max 81)
21
# Number of Offset Waterlines (columns) (odd integer: min 5, max 81)
21
# Ship Loading Type
3
# Ship Loading Formula Parameters
1.0,0.0,0.0
# ===== WAVE ELEVATION PARAMETERS =====
# Sectorial Cuts and Patches
# R0
5.0
# R1
20.0
# Beta
22.5
# Nr
101
# Nbeta
101
# Rectangular Cuts and Patches
# x0
200.0
# x1
500.0
# y0
-300.0
# y1
300.0

```

```

# Nwx
301
# Nwy
301
# Beaches and Walls
# x0
5.0
# x1
20.0
# y0
7.5
# z0
-5.0
# z1
0.0
# Slope
90.0
# Nbx
2
# Nbz
2
# ===== FIRST HULL =====
# Offsets
-1
# Displacement Volume (cubic metres)
166124.139
# Length (metres)
360.788
# Draft (metres)
14.0
# Longitudinal Separation (metres) (0.0 for a monohull)
0.0
# Lateral Separation Distance (metres) (0.0 for a monohull)
0.0
# Loading Type for this hull
3
# Loading Formula Parameters
1.0,0.0,0.0
# Trim Method
0
# Trim: Number of speeds ( >= 2)
2
# Trim: speed, angle
0.0,0.0
10.0,0.0
# Sinkage Method

```

0
Sinkage: Number of speeds (≥ 2)
2
Sinkage: speed, amount
0.0,0.0
10.0,0.0
Heel Method
0
Heel: Number of speeds (≥ 2)
2
Heel: speed, angle
0.0,0.0
40.0,0.0
Appendages (0=None)
0
Other Particulars (0=None)
0